University of Colorado - Boulder

ASEN 4018 - Senior Projects

# OSPRI


Author:
William Watkins

Author:
Dishank Kathuria

Author:
Harrison Methratta

Author:
Joseph Derks

Author:
John Wissler

Author:
Timothy Breda

Author:
Ryan Joseph

Author:
Michael Vogel

Author:
Joshua Seedorf

Author:
Zakhar Dmitriyev

Advisor:
John Mah

College of Engineering & Applied Science
UNIVERSITY OF COLORADO BOULDER

# Contents

# List of Figures

## List of Tables



## Nomenclature

$\dot{m}$ = mass flow [kg/s]
$v$ = velocity [m/s]
$A$ = area [m$^2$]
$A_e$ = exit area [m$^2$]
$\rho$ = density [kg/m$^3$]
$D$ = diameter [m]
$L$ = length [m]
$P_0$ = total pressure [Pa]
$P$ = static pressure [Pa]
$P_e$ = static pressure at exit [Pa]
$P_\infty$ = room static pressure [Pa]
$T$ = thrust [N]
$F$ = force [N]
$M$ = moment [N $\cdot$ mm]
$\sigma_b$ = beam stress [N/mm$^2$]
$I_y$ = cross sectional moment of inertia [mm$^4$]
$\sigma_0$ = Standard deviation of load cell zero values [lb]
$\sigma_5$ = Standard deviation of 5.30 lb calibration trials [lb]
$\sigma_{10}$ = Standard deviation of 10.06 lb calibration trials [lb]
TSFC = Thrust Specific Fuel Consumption
AFRL = Air Force Research Laboratory
APOP = Aerospace Propulsion Outreach Program
AFB = Air Force Base
CFD = Computational Fluid Dynamics
kRPM = Kilo Revolutions Per Minute
SLA = Stereolithography

# 1 Project Purpose and Overview

THE P100-RX is a micro turbojet engine developed by JetCat. It is a popular propulsion platform for many small-scale fixed-wing UAV applications. Weighing only 2.38 lbs, it is capable of supplying 22.5 lbf of thrust at 156,000 RPM. Its power-to-weight ratio is superior to traditional propeller-driven propulsion systems. In order to maximize freestream air entering the engine, this off-the-shelf engine is commonly mounted offset from the airframe centerline. Integrating the engine into the fuselage would reduce the exposed surface area and overall drag. This requires diverting freestream airflow into the engine intake via an inlet duct.

Well-designed inlet ducts for aircraft with non-podded engines are of interest to the aviation community. The Lockheed P-80 Shooting Star was a first-generation jet-powered fighter aircraft that integrated a single jet engine into the fuselage. It utilized a bifurcated S-duct inlet that directed airflow to the engine inlet (Figure 1). Modern military aircraft such as the F-22 and F-35 also utilize S-duct inlets.


Figure 1: Lockheed P-80 on Tarmac.

The thrust requirements for transport category aircraft are much different than those required for fighter aircraft, which is reflected in the number and types of engines they utilize. There have been several successful three-engine (trijet) commercial aircraft, including the Boeing 727 and Lockheed L-1011. Both of these aircraft utilized an internal, centerline-mounted engine mounted in the tail of the aircraft. Like the military aircraft mentioned above, an S-duct inlet was required to direct airflow to the inlet of the centerline-mounted engine. (Figure 2)

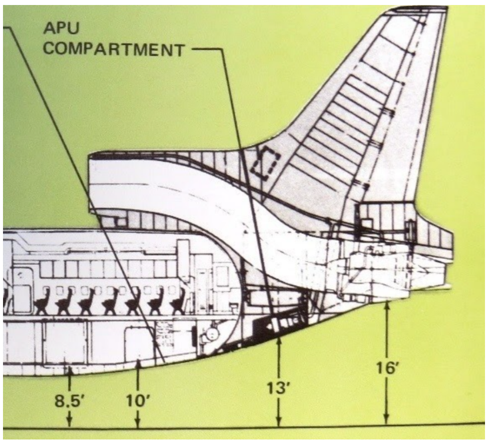


Figure 2: Lockheed L-1011 with Center Mounted Engine in the Tail.

The goal of the OSPRI research and development project is to design and build a low-loss serpentine duct inlet, offset from the compressor face of the engine, with minimal thrust and total pressure losses. Specifically, the project's goal is to develop an S-duct inlet for the JetCat P100-RX engine with a minimum of a 6-inch offset from the engine centerline, and to design and build a test rig capable of measuring the total pressure recovery of the inlet. Total pressure losses below 2% between the inlet exit and freestream, and a reduction of thrust output and increment of Thrust Specific Fuel Consumption (TSFC) below 5% are customer objectives for engine performance with the inlet modification. In addition, the inlet design should reduce axial distance from inlet entrance to exit, reduce compressor face pressure distortions, and minimize manufacturing and modification costs. If successful, this project will enable the integration of the JetCat P-100RX into the fuselage of future UAVs.

## 1.1 Previous Work

The Air Force Aerospace Propulsion Outreach Program (APOP) is sponsored by the Air Force Research Laboratory and began in 2010 for the purpose of engaging undergraduate engineering students in the study of gas turbine engines. Each year participating undergraduates are tasked with designing, building and/or modifying a different aspect of a JetCat turbojet engine. Universities across the country participate in the APOP competition, with the University of Colorado, Boulder, participating in several past competitions.

In 2015, the focus of the APOP competition was to increase fuel efficiency without sacrificing thrust or significantly increasing weight. A new exhaust nozzle, optimized for supersonic flow, was the focus of the 2016 competition. In 2017, the competition focused on ignition at very low temperatures. Designing a new engine control unit (ECU) was the focus in 2018 and, in 2019, the competition focused on designing and building a thrust vectoring system, as well as developing an anti-windmilling system. This year's competition to design and build an S-duct inlet for the JetCat P100-RX engine continues the APOP's pursuit of engaging undergraduate engineering students in the study of gas turbine engines.

The S-ducted inlet has been studied in great computational detail by NASA (Figure 28). The NASA inlet design was modelled using three different approaches: an inviscid model, a viscous vortex generator model, and a viscous BAY model [1]. Each model was tested at a free stream mach number of .78. The simulations yielded data on total pressure recovery, as well as how the inlet affected the throat mach number. The results obtained from this research can be leveraged by the team, as the flow conditions are similar to what will be expected for the JetCat P100-RX. This NASA study characterizes subsonic, viscous, and compressible flow which is the flow regime our team will be dealing with for the project. The values tabulated in their results can be used to inform our design and establish a baseline for our initial design choices.

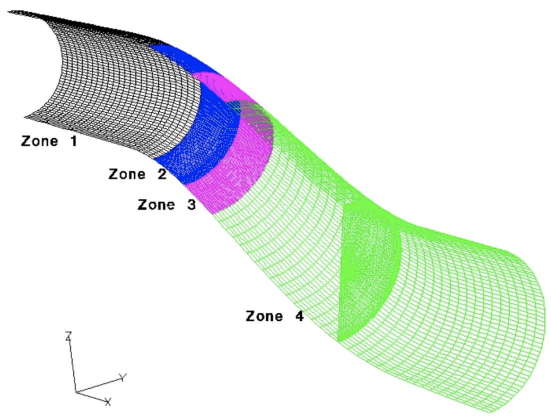


Figure 3: NASA S-Duct Inlet Design

| Case | No. Iter. | AIP Total Pressure Recovery | Throat Mach Number |
|---|---|---|---|
| Experiment | | 0.9735 | 0.7009 |
| Gridded Vanes | 30000 | 0.9775 | 0.6620 |
| Wendt Model | 20000 | 0.9871 | 0.6888 |
| BAY Model | 20000 | 0.9778 | 0.67153 |

Figure 4: Results of NASA S-Duct Simulations

Previous work in the area of testing equipment and methodologies for experimental inlet analysis is readily available for most industry scale engines, however, only a small amount of research is directly relevant to the inlets and engines of similar scale to the project's system. The paper "Flow Characteristics of an Ultracompact Serpentine Inlet with an Internal Bump" goes into detail on the experimental methodology and equipment utilized for pressure measurements within the inlet [11]. The paper details the problem of flow seperation in an S-duct of our scale, describing its most common location at the second turn of the inlet, forming two counter-rotating vortices. The team utilized a total pressure rake and a series of surface static taps to characterize the flow structure in the inlet. The rake was placed at the inlet exit to analyze the pressure distribution where the compressor face would be in an integrated engine. The static ports were placed along areas of the inlet where flow was expected to produce adverse boundary layers or separation, primarily the surfaces of the first and second turns.

Similar methods of static surface taps have been utilized by a variety of other teams to analyze the flow characteristics of numerous inlets [12] [13] [14]. Furthermore, the most frequently utilized method of gaining detailed pressure distortion and flow structure measurements are total pressure rakes placed where needed [15]. This project utilized these methods in order to develop a boundary mitigation system for an inlet highly integrated into an airframe.

# 2 Project Objectives and Functional Requirements

Table 1 outlines the levels of success for this project. Since the JetCat P100-RX engine can be unreliable, the lower levels of success focus on the correct operation of the test rig and the pressure recovery in the inlet, but do not include operation of the engine. Higher level objectives focus on the operation of the engine in conjunction with the inlet, and the performance requirements as outlined by AFRL.

Table 1: Specific Objectives and Levels of Success.

| Level | Objectives |
|---|---|
| 1 | A test rig is designed and manufactured that is capable of interfacing with the inlet and engine mounts and measuring inlet performance metrics at discrete locations along the inlet length, the inlet entrance and the compressor face. |
| 2 | Experimental verification of test apparatus accuracy using a diffuser test piece with known theoretical pressure and velocity characteristics using a flow surrogate. |
| 3 | Experimental verification of inlet's total pressure recovery below 90% across the full simulated RPM range of the engine using a flow surrogate. |
| 4 | Experimental verification of nominal engine operation over full RPM sweep with inlet attached, meeting level 3 objectives, increasing TSFC by no more than 10%, and decreasing thrust by no more than 10%. |
| 5 | Experimental verification of nominal engine operation over full RPM sweep with inlet attached, with total pressure recovery $\leq$ 98%, TSFC increased by no more than 5%, and thrust decreased by no more than 5%. |

## 2.1 Functional Requirements

The design of the S-duct inlet for the JetCat P100-RX engine is a self-contained project and does not rely on a larger system, nor does it fit into other design problems. The requirements for the inlet design project stem primarily from the AFRL/APOP competition scoring material. The team will design an inlet for use with the JetCat P100-RX that will produce the desired solution to the requirements and a custom built test rig that will provide total pressure data. The horizontal CU Aerospace engine test stand will provide thrust data. Specifically, OSPRI will meet the following functional requirements:

Table 2: Functional Requirements.

| Req | Description |
|---|---|
| 1 | Design and build an S-duct inlet for use with the JetCat P100-RX turbojet engine that performs according to the customer objectives. |
| 2 | Design and build a test apparatus to measure critical inlet performance metrics and inform inlet design. |

## 2.2 Concept of Operations

The CONOPs for this project were designed in order to streamline the design, manufacturing, and testing of the inlet.The S-Duct and the test apparatus will first go through a design and build phase. During this phase, multiple conceptual designs of the inlet will be developed followed by the CFD analysis and model verification. The inlet will then be manufactured to initiate testing. In the case of test apparatus, it will be designed and assembled followed by sensor calibration to ensure the accuracy of the results. After the design and build phase, there will be a testing phase. During the testing phase the designed inlet/inlets will first be tested on the designed test apparatus. Once the results from these tests match the design criteria ($>$ 98% Pressure recovery), the inlet will move on to engine testing. For the engine test, the selected inlet will be attached to the engine face using a transition piece provided by the AFRL and run over a full RPM sweep. Pressure data will be recovered in order to ensure the inlet performs as expected. Lastly, if the inlet passes the final engine test, the designed inlet will then move on to compete in the APOPs competition at Wright Patterson Air Force Base in Ohio.

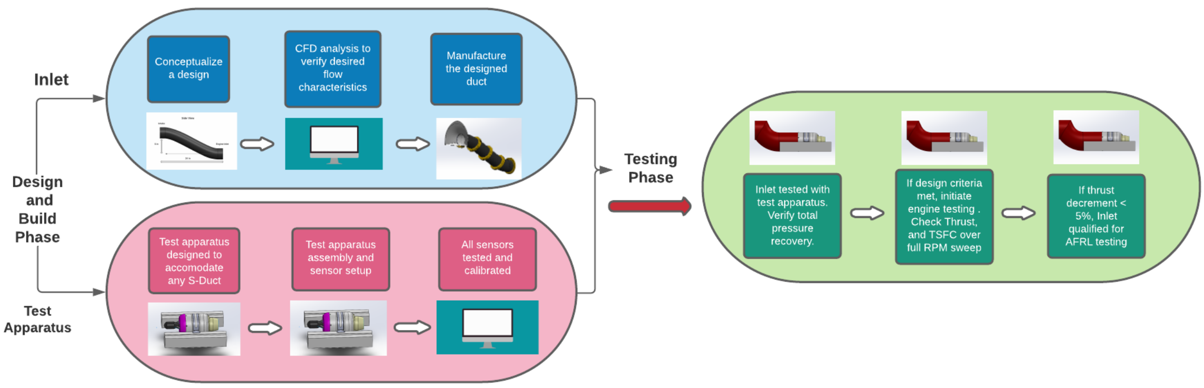


Figure 5: Ground Testing ConOps.

# 3 Final Design

## 3.1 Functional and Design Requirements

The functional requirement for team OSPRI's project at the most basic level was to design, build, and validate an S-duct inlet for use with the JetCat P100-RX turbojet engine that performs according to AFRL's objectives. For the APOP competition, AFRL created a set of design requirements in which each team must center their inlet design around. These included having a 6 inch offset from the bottom lip of the duct to the center-line of the inlet exit. This requirement was at the focus of AFRL due to the desire to integrate the inlet with a UAV which would have an inline engine mount, requiring the need for air to be guided from the surroundings into the compressor of the engine safely. AFRL also outlined that a shorter inlet would be scored higher, since having a shorter inlet would most likely reduce weight and increase the performance of the aircraft. With a short, 6 inch offset inlet, the sharp turns within the duct can cause severe flow separation which would lead to total pressure losses by the time air has reached the tubrojet compressor. A loss in total pressure at the compressor would also decrease the performance and overall thrust output of the JetCat. For this purpose, AFRL outlined that the inlet shall maintain $\geq 98\%$ total pressure and both $\leq 5\%$ thrust decrement and $\leq 5\%$ thrust specific fuel consumption.

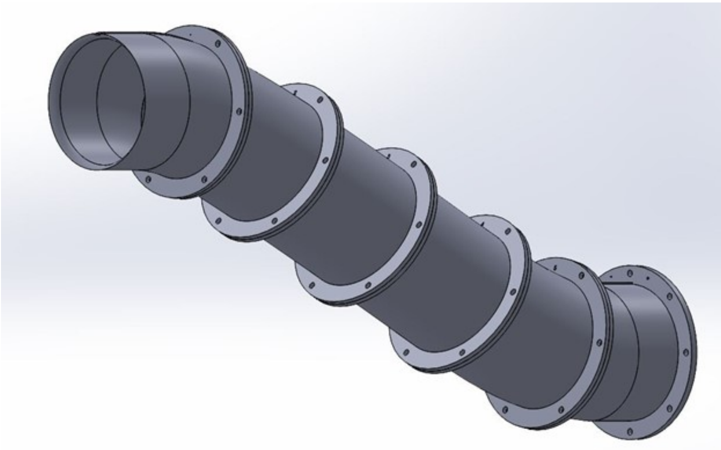

Figure 6: CAD of Inlet Final Design

## 3.2 Design Description

The inlet final design was determined an assembly of 6 flanged, sectional pieces and was a replica of the baseline design testing inlet, with some minor modifications. The modifications included removal of the pitot-rail since pressure data would not be gathered axially at AFRL. Another modification was the addition of small numbers printed on each sectional for organization and ease of assembly. The final assembly is 24 inches long axially, with a 4 inch diameter, circular cross section. This circular cross section would help with the ease of manufacturing and also distribute airflow uniformly throughout the duct to prevent pressure distortions along the cross section. The flanges on each sectioned piece not only help with assembly, but also help to support the structural weight of the duct and distribute loads which could deform the inlet if not supported. The flange on the inlet exit sectional piece is designed to integrate with the JetCat transition piece, as given by AFRL. 7 M5 bolts and nuts are used at each interface between sections, for a total of 42 M5 bolts and 42 nuts of the same size.

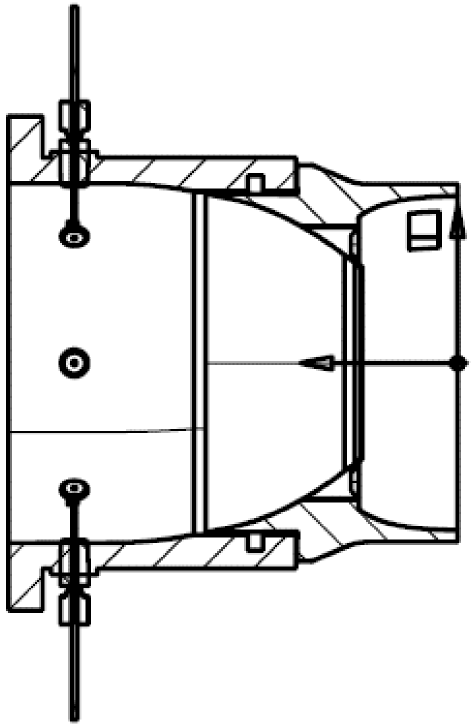

Figure 7: AFRL Transition Piece Cross Section

The printed and assembled inlet is designed to be mounted onto the testing apparatus, held by the support cradles, and interfaced with the AFRL designed JetCat transition piece. The JetCat transition piece is integrated with the JetCat P100-RX mini turbojet which is bolted to the test stand in the University of Colorado Boulder Aerospace Engine Test Cell Lab. The intended operation of the inlet is to be done safely with the JetCat initiated at an idle speed of 44 kRPM and slowly increasing kRPM so that flow within the duct can avoid turbulence or sever separation while transitioning to higher airspeeds. The final designed inlet reduces flow separation by gradually

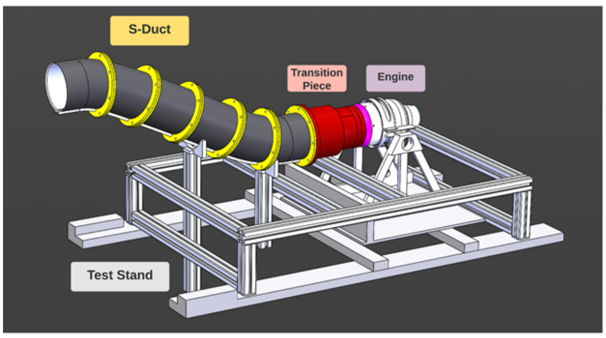


Figure 8: Final CAD Assembly Integration

#### 3.2.1 CFD Design

The final design took into consideration iterative data gathered from our CFD analyses. Those CFD analyses were of varied inlet designs, concerning our main design variables of the inlet. To reiterate, these design variables were length, entrance to throat ratio, and throat to exit ratio. During the CFD analyses processes, we were able to determine geometry that best facilitated our objectives of high total pressure recovery and low turbulence or flow disturbance. These design variables were long inlets with 1-to-1 ratios of both the entrance and exit as compared to the throat. This eventually turned into the final design of the inlet (Figure 9).

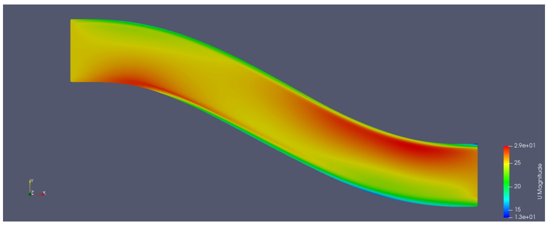


Figure 9: CFD Velocity Magnitude of Design 62 (Final Design)

Our CFD was set up for incompressible turbulent flow, as the Reynolds number of the inlet using the pipe formula ($\mathrm{Re} = U\frac{D_h}{\mu}$) was estimated to be approximately 120,000 (turbulent). For openFOAM, our CFD software, the solver they use for the incompressible, turbulent flow case is the SIMPLE (Semi-Implicit Method for Pressure-Linked Equations) algorithm. This leads to a steady-state solution for our inlet. Because the flow is incompressible, our CFD does not model total pressure loss from the flow itself, but rather from the build-up of the boundary layer along the inlet walls. this is one reason that our CFD does not line up perfectly with our actual results.

However, we made sure to verify the final design of our inlet using a mass flow surrogate, the electric ducted fan (EDF). This allowed for more precise and faster measurements of our inlet than compared to with the jet engine. Our mass flow surrogate testing with the EDF verified that we were on the right track with our design and that it satisfied all the requirements of AFRL. After testing with the EDF, we also tested with the jet engine to verify both our EDF and again our CFD data. Testing confirmed our data and the functionality of the inlet.

### 3.3 Test Apparatus Design

In order to effectively test and evaluate the inlet, a structural supporting testing frame was needed. This testing frame has been designed so that it not only supports and secures the inlet, but also facilitates the physical testing of the inlets. Two different types of tests was conducted, one utilizing a mass flow surrogate with the Electric Ducted Fan (EDF), and another with the actual JetCat turbine engine. Testing of inlets was conducted first with the EDF to gather preliminary data and ensure the team understands the internal aerodynamics before testing with the more expensive JetCat turbine engine.

Due to a limited budget, it was decided that there would be only one test frame. Only constructing one frame lead to a few different issues. The first of these issues was that the inlet frame needs to be modular to accommodate a variety of different inlets as an iterative testing procedure will take place. The second large issue with the single inlet test stand meant that the frame's design had to accommodate testing with not only the EDF, but also needed to accommodate testing with the JetCat turbine engine, interfacing with the horizontal test stand in the CU Boulder Aerospace engine test cell. The dimensions for the pre-existing horizontal test stand can be seen below in Figure 10. The horizontal test stand was measured and replicated in CAD to ensure the team could be accurate while working remotely.

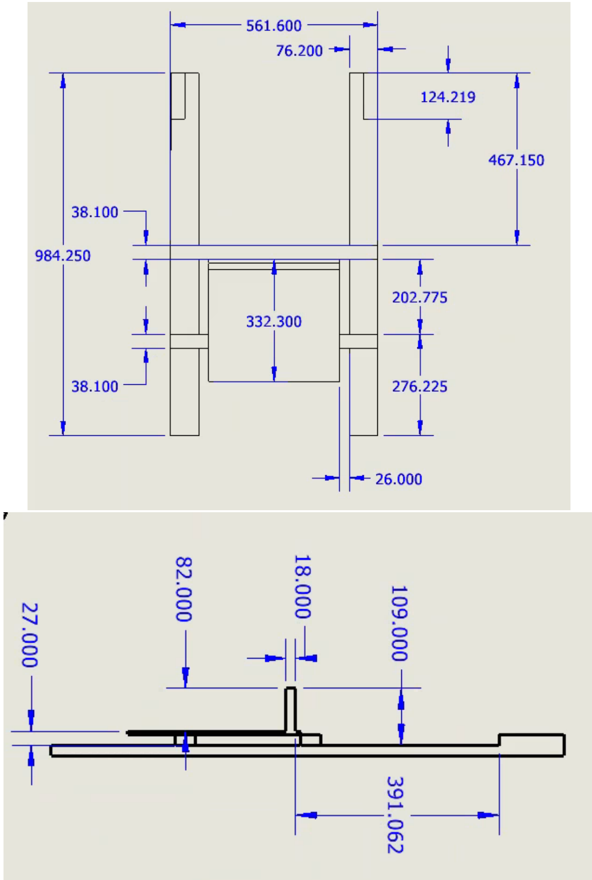


Figure 10: Engine Test Cell Stand Dimensions

The largest challenge in designing the inlet test frame is the dimensional constraints that needed to be meet in order to interface with the horizontal turbine test stand. Below in Figures 11 and 12 are initial concepts for how the inlet test frame would fit with the turbine test stand (dark grey in color). In Figure 12 it is much easier to see the two biggest dimensional challenges. The first of these was the length of the inlet test frame. If too long, then the frame would run into the elevated brackets in the front of the turbine test stand (seen on the bottom right side of Figure 12) and introduce error into the integrated load cell that collects turbine engine thrust data. The second challenge was the vertical clearance of the inlet frame over the turbine stand's middle plate. This middle plate rose approximately 109 mm from the base of the turbine stand forcing the inlet frame to rise above.

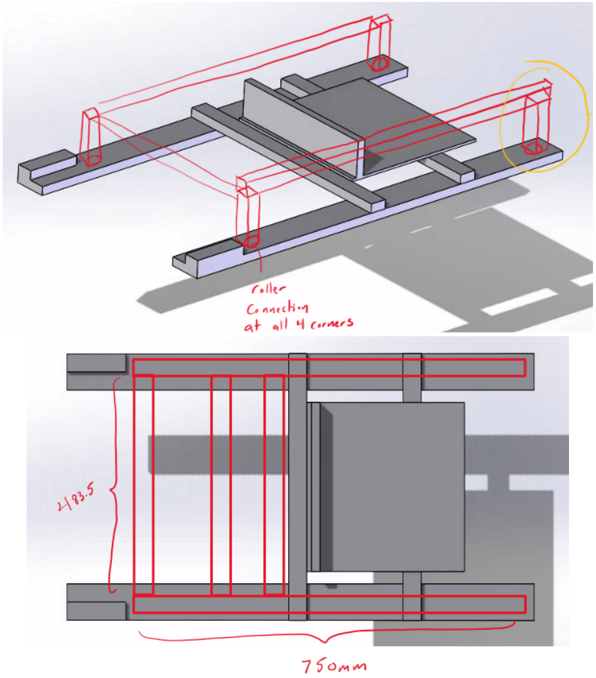


Figure 11: Inlet Test Stand Concept Drawing

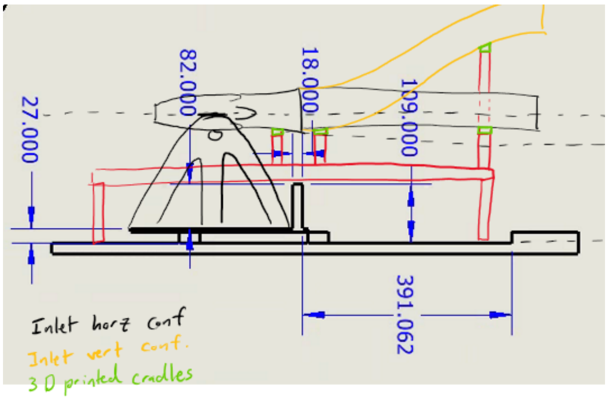


Figure 12: Test Stand Concept Side

Early on in the design process, aluminum 30x30 extrusion material was decided to be used for the inlet test frame due to its versatility, availability, affordability, and strength. With the special trapezoidal channels cut into the aluminum along with the associated trapezoidal nuts that are designed to operate in those channels, the test frame becomes extremely modular allowing any piece to simply be unbolted, and slid into any other desired position. This feature was heavily exploited in the design of the frame and the associated inlet supports as can be seen in Figure 13. Each inlet support was designed so that it can move in three different axis to accommodate any inlet offset, and inlet dimension, and any inlet orientation. The vertical sections of the inlet frame were sized for the maximum dimensions of offset that was specified by the customer for the inlet. These lengths were then added to by 3 cm to ensure that there would be a factor of safety and that any inlet would be able to be tested on this test frame. The final dimensions of the inlet test frame can be seen below in Figure 14.

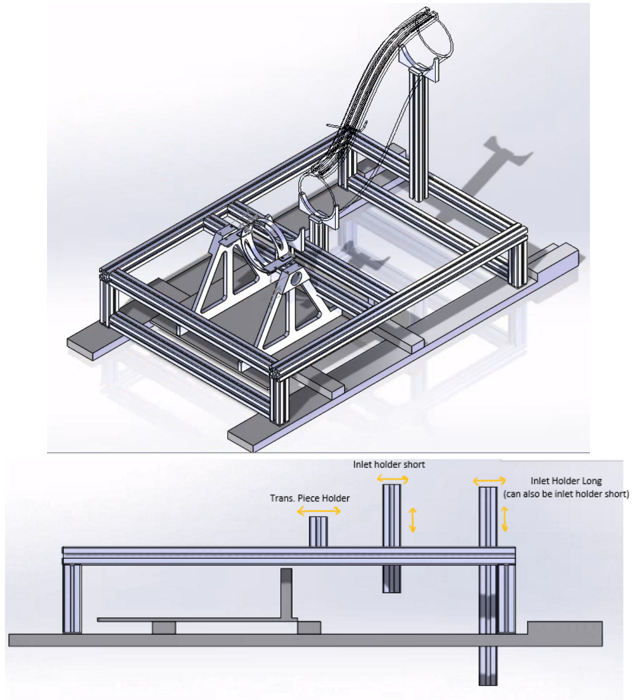


Figure 13: Final Inlet Stand on Engine Test Cell Stand

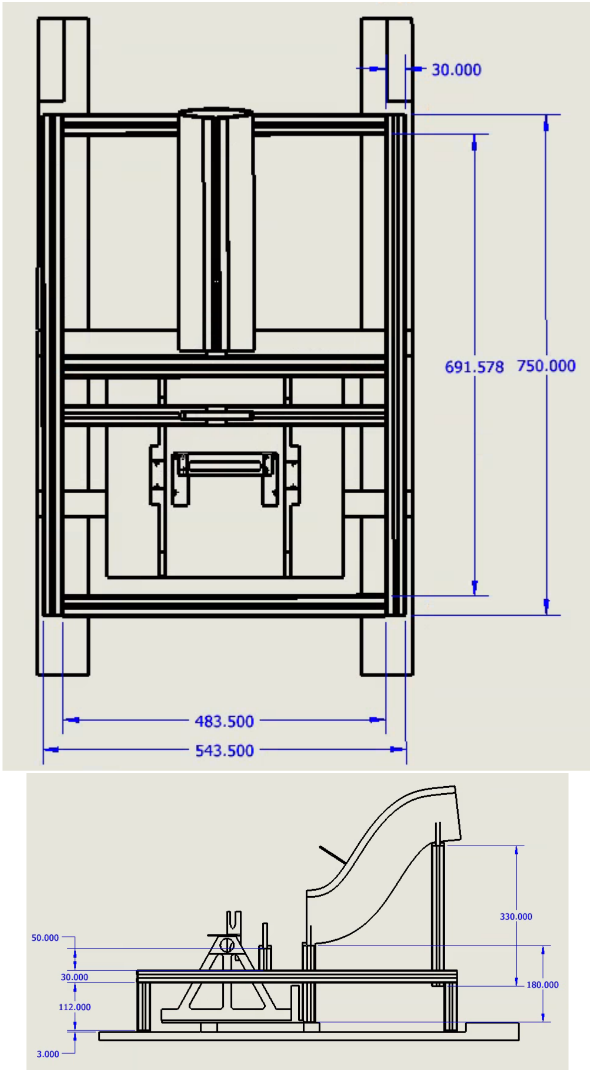


Figure 14: Final Test Stand Dimensions

With the dimensions finalized so that the inlet test frame interfaced with the turbine horizontal test stand, integration of the EDF testing assembly onto the test frame needed to be accomplished. It was decided that the EDF was to be secured to the inlet test frame via vertical aluminium extrusion pillars. These pillars were dimensioned at 12 cm in order to put the EDF at approximately the same height as the JetCat turbine engine would be when testing with the horizontal turbine test stand. This design decision was made to ensure that the previously found vertical inlet support lengths would be able to work with both tests. The EDF was placed on a sliding rail so that it could easily be changed in and out for the different tests. The inlet test frame in the EDF test configuration can be seen below in Figure 15.

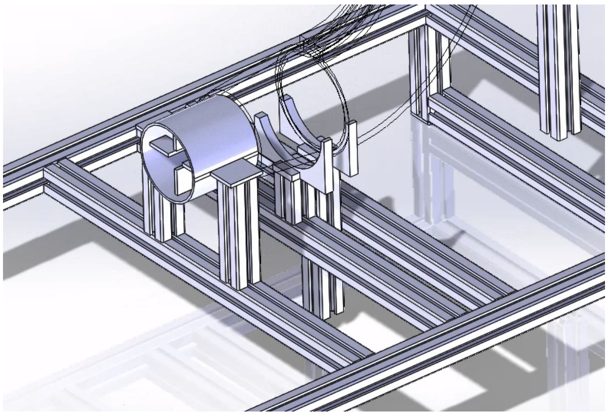

Figure 15: EDF Integrated Test Stand View

With the EDF placed on two 12 cm pillars, the team was worried about the bending moment of the 30x30 aluminum extrusion material. A simple bending analysis with the flexure formula (see equation 2) was conducted on the 12 cm long aluminum bars to ensure that there would be no issues. The selected 80 mm EDF (see more in the mass flow surrogate section below) specifies that 2.45 $kg$ of thrust can be produced. A factor of safety of 1.25 was used which lead to a thrust of 3.0625 $kg$ for the analysis. Documentation from the aluminum extrusion manufacturer reported a cross sectional moment of inertia to be $I_y = 2.83 \cdot 10^4\ mm^4$ and the y dimension to be $y = 30\ mm$ [21]. The calculations below are for only a single aluminum pillar.

$$\text{F} = 3.0625 \text{ kg} = 30.0329 \text{ N}$$

$$Moment = Force \cdot Distance = 120mm \cdot 30.0329N = \mathbf{3603.944\ Nmm} \tag{1}$$

$$\sigma_b = \frac{M \cdot y}{I_y} = \frac{3603.944\ Nmm \cdot 30\ mm}{2.83 \cdot 10^4\ mm^4} = \mathbf{3.8204\ N/mm^2} \tag{2}$$

For the aluminum 30x30 extrusion material, the manufacture reports a longitudinal elastic modulus of 69972 $N/mm^2$, a tensile strength of 245 $N/mm^2$ and a proof stress of 205 $N/mm^2$ [22]. From the results of the calculations in equation 2 above, the forces of the EDF on the two 12 cm pillars were well within the capabilities of the selected aluminum extrusions.

Once everything was properly analyzed and dimensioned, the design was finalized and the raw materials were ordered pre-cut from manufactures. Ordering pre-cut materials reduced the overall construction and assembly time of the frame, allowing for the team to start testing with both the EDF and JetCat sooner.

After testing began with the designed test frame integrated onto the horizontal JetCat engine test stand, the team was unable to collect reliable thrust data. After analysis it was determined that the friction between the test frame and the horizontal engine test stand was contributing to error in this measurement. To resolve this, the frame was removed and a support for the AFRL transition piece was fashioned. More info on this issue and solution can be found in section 5.3.3.

# 4 Manufacturing

## 4.1 Inlet Manufacturing

Inlet production and assembly that could be done quickly and hassle-free was the focus of the manufacturing plan. Knowing there would be multiple inlets manufactured in an iterative process would mean the team should also keep lower-priced methods in mind as well. For these reasons, 3D stereolithography (SLA) printing was chosen to be the method for the 6 inlet pieces, along with the JetCat & EDF transition pieces which would be necessary for preliminary verification testing. The FormLabs 3B SLA printer in the University of Colorado Aerospace building was utilized for printing each of the inlet sectionals and transition pieces with 100 micron resolution. The 6 inlet sectional pieces sport wide flanges which inhibit the ability of the pieces to be assembled with 7 M5 bolts and nuts at each interface.

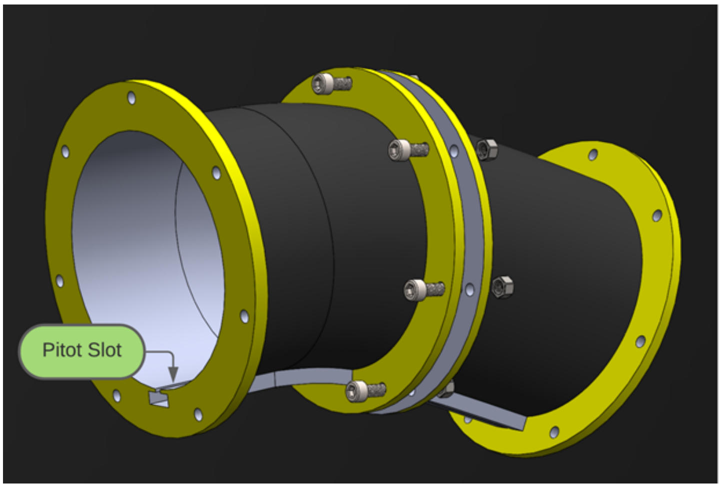


Figure 16: CAD of Inlet Sectional Assembly

Using the properties of the chosen SLA resin, FormLabs standard, a series of stress and vibration test were conducted using SolidWorks. Vibration tests indicated that a 24 inch inlet supported on both ends as well at the center would not fail until a frequency of 950 Hz (Figure 17)

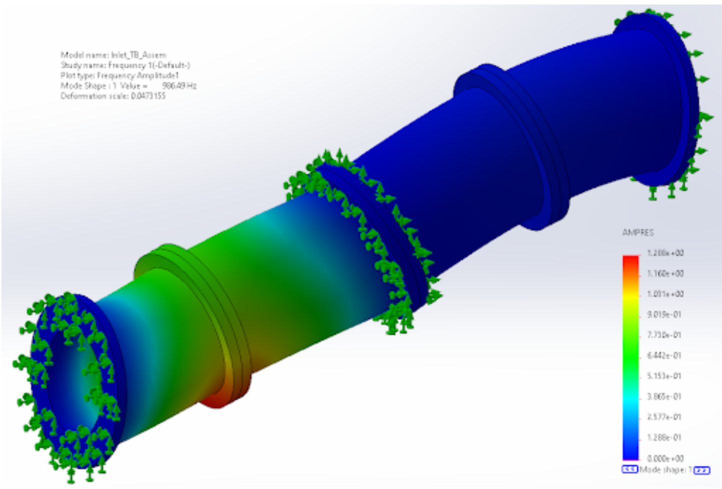


Figure 17: Inlet Failure due to Vibration

In addition to the vibration test, a free-standing static test was also conducted using SolidWorks. The results of the test are shown below (Figure 18); however, it should be noted that the displacement shown is highly exaggerated and that the stress did not reach yield.

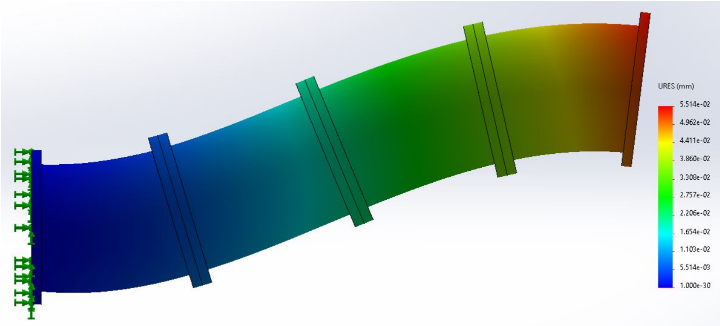


Figure 18: Inlet Static Test

The SLA printing process requires inserting dense support structure into large cavities, such as within the duct portion of the inlet, which prevents cracking and deformations during the printing process. While necessary for the manufacturing of the sectional print, the support structure was removed prior to assembly and testing (Figure 19). Wire-cutters were used for the removal of the bulk of the support structure, after which the innner surface of the duct was sanded in order to remove any residual pieces. A smooth inner surface was required as to not disrupt surface-flow interactions, which could result in a more turbulent boundary layer and thus greater total pressure loss within the inlet. Following post processing, the inlet sections were assembled and attached to the AFRL-provided transitional piece (Figure 20). Challenges overcome with inlet manufacturing included resizing thru-holes with drill bits, epoxying cracks formed during printing, and using foil HVAC tape along with modelling clay to close any gaps where air could escape and lead to unwanted flow losses.

Figure 19: Pre-and-Post-Processing SLA Inlet Sectional

Figure 20: Fully Assembled Inlet

## 4.2 Test Apparatus Manufacturing

### 4.2.1 Sensors and Data Collection

The designed measurement apparatus needed to be capable of calculating total pressure, as well as have the ability to map the pressure distributions within the duct. To meet the project functional requirements, the OSPRI team needed to verify that a selected inlet design can perform within the 98% pressure recovery metric. In order to gather these measurements, a Scanivalve DSA 3217 module was used in conjunction with a pitot-static probe. Via the pitot rail system, pressure measurements could be taken from any point along the center-line of the inlet length with two degrees of freedom.

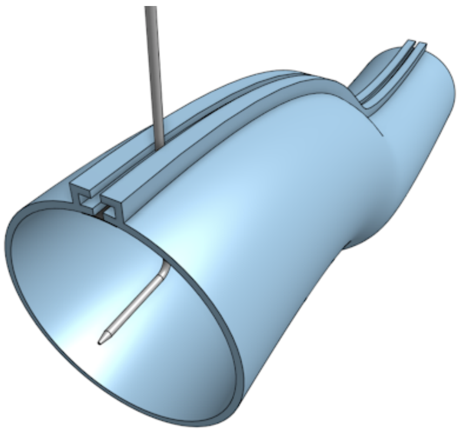

Figure 21: Pitot Slotted Rail System

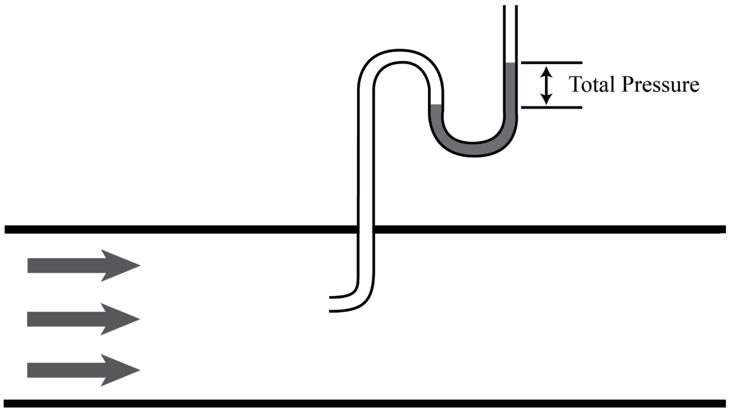


Figure 22: Total Pressure Computation

The DSA module itself was connected via ethernet cable to team OSPRI's computers for data acquisition and processing. In order to read this data appropriately, Scanivalve DSA software was installed locally on the computers. The DSA module has a particular IP address that must be configured with the host computer in order for the module to function properly. Upon successful connection between the computer the the DSA, team OSPRI was able to gather and organize the desired pressure data for post-processing. The module had 16 pressure channels as well as a reference channel. Since total pressure recovery was the main objective for means of analysis, only a single main channel was needed on the DSA. Our tests were conducted with the reference channel connected to the static port, and channel 1 connected to the total pressure port. The Scanivalve was an incredibly crucial device that allowed team OSPRI to conduct and complete all subsequent testing with the JetCat and the designed inlet.

#### 4.2.2 Modular Frame

The frame which supported the inlet had to be highly modular in design to be able to accommodate multiple different inlets as well as to allow the JetCat engine and EDF to be mounted interchangeably. Since the Engine Test Cell already contained a secure structure on which to mount the JetCat, the test frame needed to be designed to integrate with the existing support structure. A preliminary design of this interface is shown in Figure 23. Measurements were taken of the existing structure, and a rectangular test frame was designed.

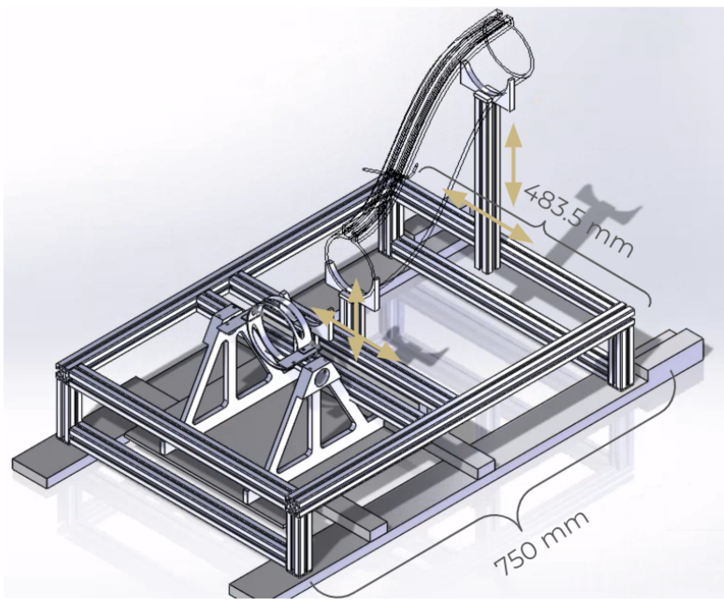


Figure 23: Test Apparatus and Support Structure Interface

The final design has two adjustable vertical supports each connected to horizontal rails that can be positioned up and down the length of the stand. Again, this modular design allows for the attachment of any sized inlet that is seen fit for testing. Adjusting the vertical supports allow for adaptation to various axial offset distances while the horizontal sliders allow adaptation to inlets of varying lengths.

The test frame was constructed out of 3030 aluminum extrusions (30 mm x 30 mm cross section). This material is standard in engineering for rapid prototyping and construction of frames as the material is cheap, lightweight, rigid, and highly standardized in its construction and accessories. All aluminum for the project was ordered through MISUMI, an online retailer which can send aluminum extrusions cut to exact millimeter specifications. With this convenient retailer, the team ordered all aluminum extrusions exactly as had been designed in CAD, and used standard 90 degree angle brackets, aluminum extrusion insert connecting nuts, and M5 bolts to finalize construction. All of the custom parts for the frame such as those connecting the frame to the JetCat, EDF, and inlet were designed in OnShape and 3D printed on a Lulzbot Mini in PLA to ensure precise fitment as well as rigidity and strength between the inlet and the test equipment.

The connections between the test frame and the test equipment can be broken down into three parts: the inlet cradles, transition piece connectors, and EDF connector. All three of these parts were designed to fit into the open cross-section of a piece of 3030 aluminum extrusion to ensure a tight fit. The inlet cradles were minimalist in design and consisted of merely a U-shaped cradle for the inlet to rest on during testing. Not much, if any, lateral or axial loads were expected to be placed on the inlet itself, so a simple vertical support was enough to ensure safety in this area. There was a cradle designed to connect to both the transition pieces used in the project. The piece designed to connect to the AFRL provided transition piece from the inlet to the JetCat utilized a design which allowed hose clamps to be inserted and for the piece to be screwed down to the base to ensure secure connection. The transition piece from the inlet to the EDF was designed with mounting flanges. The connector piece was designed to fit to the holes on these flanges and be secured with nuts and bolts. Similarly, the connector for the EDF was designed to fit to the contours of the EDF and mount to the provided mounting holes on the housing of the EDF. The three categories of pieces (four total pieces) are shown below.

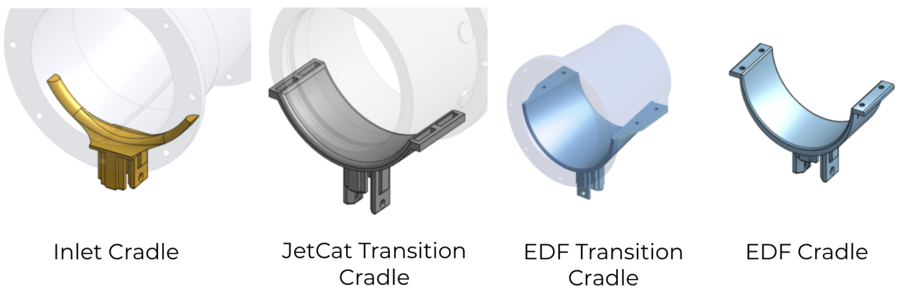


Figure 24: 3D printed Cradles  Connectors

The existing engine support structure was outfitted with a load cell that the team would use to collect thrust data from the engine and EDF. This load cell relied on the engine being mounted to a platform on frictionless linear bearings. This provided the added design challenge of making the test frame able to slide, or at least to have a bit of give opposite the direction of the thrust. The design incorporated four hard plastic caps where the frame rested on the existing aluminum support structure. The intention was for these pads to reduce the static friction coefficient of the test frame on the support structure. In practice, this proved somewhat problematic and the thrust data was not as expected in initial tests. This problem was fixed by designing and 3D printing a temporary support beam to hold the inlet solely on the existing sliding system so as to not add friction during the thrust decrement testing. While getting this data was ultimately important to verifying our design requirements, it was only implemented for the last few tests, with the majority of test being performed on the initially designed test frame. The fully assembled test frame can be shown below.

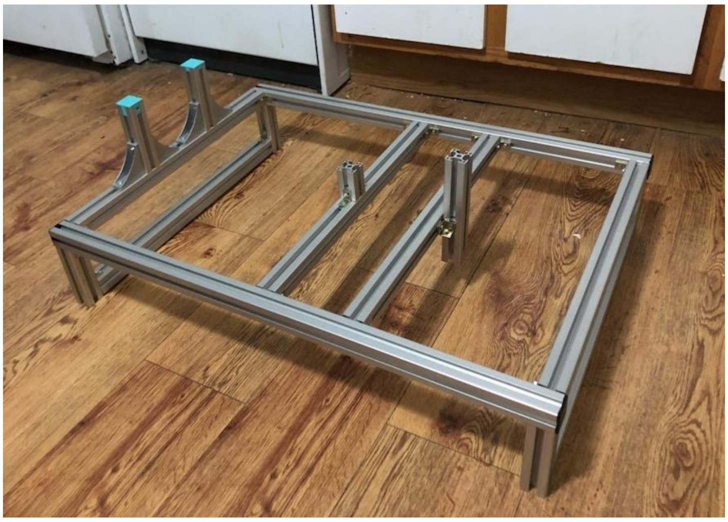

Figure 25: Test Apparatus Modular Frame

# 5 Verification and Validation

## 5.1 EDF Testing

Before initial inlet testing could begin with the electric ducted fan (EDF) its mass flow characteristics needed to be verified in order for it to act as a mass flow surrogate for the JetCat turbine. For the primary mass flow test a bellmouth inlet and a custom transition piece was designed and 3D printed. The bellmouth was used to organize the flow and prevent it from needing to turn a sharp corner during the static tests. The transition piece (seen in Fig. 26) interfaced the bellmouth and the EDF, as seen in Fig. 27. Flow data was collected via the pitot static probe which allowed for the flow speed and therefore the EDF's mass flow to be calculated.

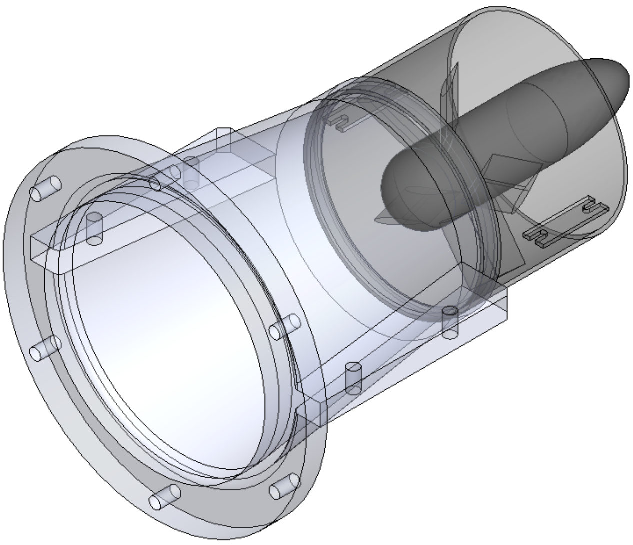

Figure 26: EDF with Transition Piece

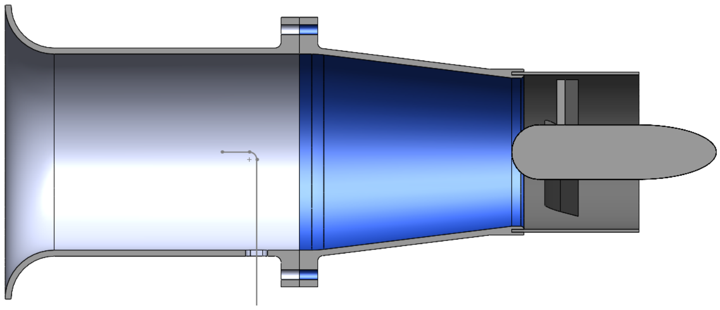

Figure 27: EDF Mass Flow Test Setup

The EDF functioned using an electronic speed control (ESC) which required a 5-12V PWM signal input between 5% and 10% to throttle the fan from between 0% and 100% thrust. This signal was generated using an Analog Discovery 2 (AD2) oscilloscope and wave generator. The output range of the AD2's wave generator has a maximum limit of 5V which was not recognized by the ESC, as such a voltage amplifier was designed using an op-amp to boost the voltage to between 5V at the low end and 9V at the high end. The circuit was independantly powered from a wall outlet through a Redboard, capable of a 9V max output. The power input for the EDF and ESC that was utilized for all tests was a 4S 5000mAh Li-Po battery.

The integrated EDF-bellmouth setup was then mounted on the Test Apparatus and readied for the test. The pitot static probe was connected to a DSA 3217 Scanivalve with static pressure as reference. Utilizing provided software from the Scanivalve website for use with the particular device, data was collected at the center of the flow. The EDF is then commanded through its throttle range. The mass flow is finally calculated from the known area and dynamic pressure within the bellmouth.

An initial mass flow test that was conducted resulted in erroneous values, appearing to have a systemic offset which was assumed to have originated from a calibration error. A subsequent test utilizing the same methodology and ensuring calibration of the pressure measurements was done adequately, generated results which were in the expected range of values.

Table 3: EDF Mass Flow Verification Results

| EDF Throttle [%] | Dynamic Pressure [Pa] | Flow velocity [m/s] | Mass flow [kg/s] |
|---|---|---|---|
| 55 | 325 | 23.88 | 0.88 |
| 75 | 450 | 28.10 | 1.04 |
| 95 | 650 | 33.77 | 1.25 |

In order for the EDF to act as a mass flow surrogate for the JetCat turbine, it needed a total mass flow of around $0.23kg/s$ (according to the manufactures specifications) at the top end of the throttle range, which we were able to verify with the results collected during the aforementioned tests.

After the mass flow of the EDF and the control and the pressure data collection setups were verified, the team went on to begin inlet testing. The primary purpose of the EDF test, as the end of the project was moving closer, was to verify that the inlet did not create adverse compressor face pressure distributions and was able to hold up to the vibration and stresses during testing in order to move to turbine testing.

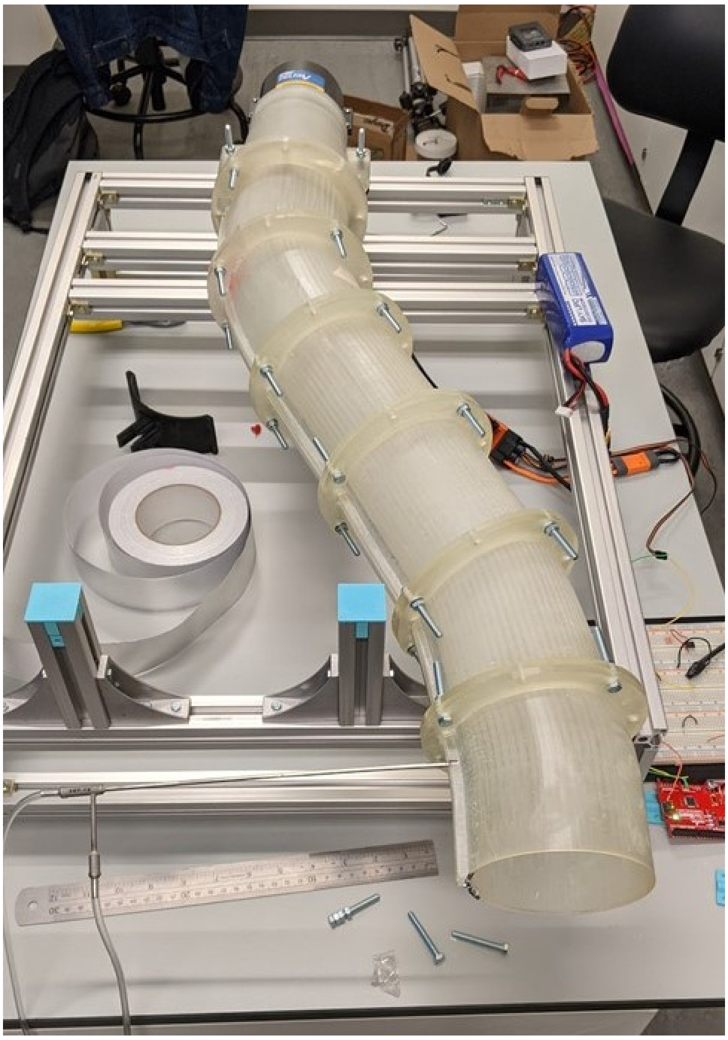

Figure 28: EDF Test Setup

## 5.2 Inlet Performance vs CFD Model Performance


Figure 29: Inlet Iterative Test Loop

Due to the immense complexities that are involved with internal flows, the verification and validation plan for the inlet was a physical iterative testing procedure. This physical testing procedure was needed as neither CFD nor analytical calculations were going to carry the accuracy needed to make important design decisions due to the complex internal flows. Because of this, testing was iterative starting first with a CFD model that could determine detriments in the designs and calculate high total pressures. From there, the process (outlined in Figure 29) started with the manufacturing of a test inlet. This was then followed by integrating the inlet with the testing apparatus and running physical tests (first on the EDF, then moving to the turbine if deemed safe and necessary) to gather data. After data was gathered and analyzed, conclusions were drawn in order to see where improvements could be made. Then the inlet was redesigned where either the existing inlet was slightly modified or a new inlet would be manufactured to start the iterative process over again.

When comparing the CFD model to the actual inlet, some discrepancies were found, as expected. In general, the CFD model was extremely optimistic, especially because of the low airspeed and conservative design of the inlet. The CFD predicted a mainly inviscid model with some boundary layer build-up, but it did not account for small turbulences around the bends of the inlet. These turbulences corrected themselves in the inlet. However, because of the low airspeeds, the discrepancies between the CFD and the actual test results were actually quite minimal, and did not significantly impact the design process.

### 5.2.1 Total Pressure Recovery for EDF testing

The total pressure recovery for the inlet attached to the EDF was 99.81%, when compared to the EDF, they are almost the same, with the EDF total pressure recovery at 99.8%. The CFD model predicted that the total pressure recovery would be approximately 99.98%. Which as mentioned before, is likely due to the model considering the flow as incompressible and only subtracting the boundary layer flow slow-down. This fullfills AFRL's requirement of having a total pressure recovery of greater than or equal to 98%.

## 5.3 JetCat Testing

### 5.3.1 Stock JetCat Engine run

One of the earliest tests that was performed in the lifecycle of this project was a stock JetCat run with no modifications, sensors, or attachments to the stand or the JetCat. This was accomplished as the previous team had issues getting the engine to properly run and also ran into reliability issues. This test turned out to be essential to the project as problems were encountered during testing and the JetCat engine needed to be sent to the manufacture for servicing twice before it would even start. It was discovered that the electric starter motor was burnt out, the internal shaft bearings were gummed up, and the front sensor board had a few components burnt out. These issues were resolved by the professional service technicians at JetCat Americas which allowed for the turbine to start up and run reliably for the remainder of the project. The stock JetCat tests ran through the entire RPM sweep (from 44k RPM to 156k RPMs) with no issues whatsoever.

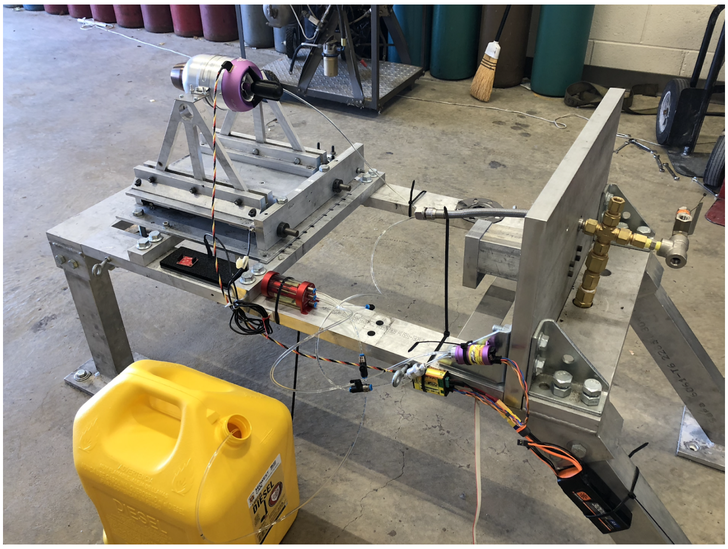

Figure 30: Stock Engine Test Setup

### 5.3.2 Massflow Verification

Next for the JetCat was the verification test of the turbine's mass flow. To accomplish this, the JetCat was fit with the AFRL designed transition piece and the bell mouth that was used in the EDF mass flow test above. The pitot static probe was then put into the flow in the bell mouth (see Figure 31) to collect the mass flow data using the same procedures that were used in the EDF mass flow test.

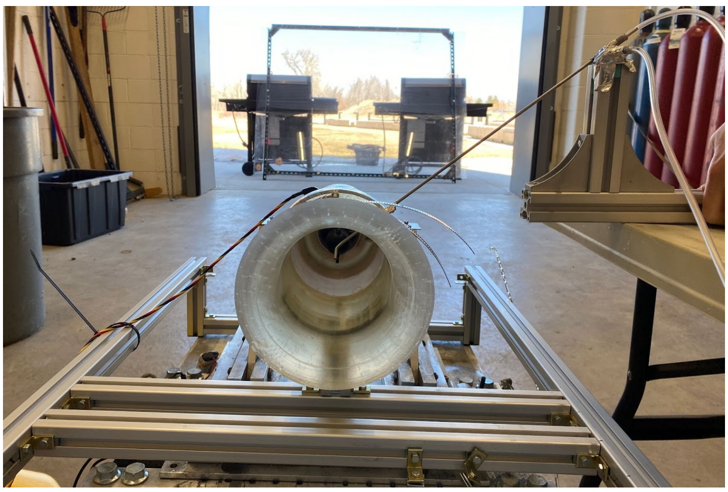

Figure 31: JetCat Mass Flow Test Setup

During this test, issues were encountered with the operation of the JetCat engine. Thrust data was collected while this test was running which can be seen below in Figure 32. From this data, it is clear to see the stair-step profile of the engine which corresponded to the different thrusts associated with different RPM levels. During the first six incremental RPM steps of the test, the JetCat was performing nominally up until 120k RPM. Once the test profile stepped to 136k RPM, the team started noticing a difference in performance. This can be seen in Figure 32 as the JetCat initially well overshot then struggled to maintain a constant thrust. While this data below shows thrust vs time rather than thrust vs RPMs, it is still a great tool for visualizing the JetCat's performance as thrust is closely related to operating RPMs. As the test progressed to the full 156k RPM, the engine exhibited an extremely unstable condition that the team has described as surging. This unstable surging can again be seen in Figure 32 at the final right most peak. It is clear to see from the thrust data that this final condition was extremely unstable and warranted an immediate test termination and engine shutdown before there was any harm or damage caused. With this information, the team set an artificial limit on testing at 120k RPMs for safety purposes.

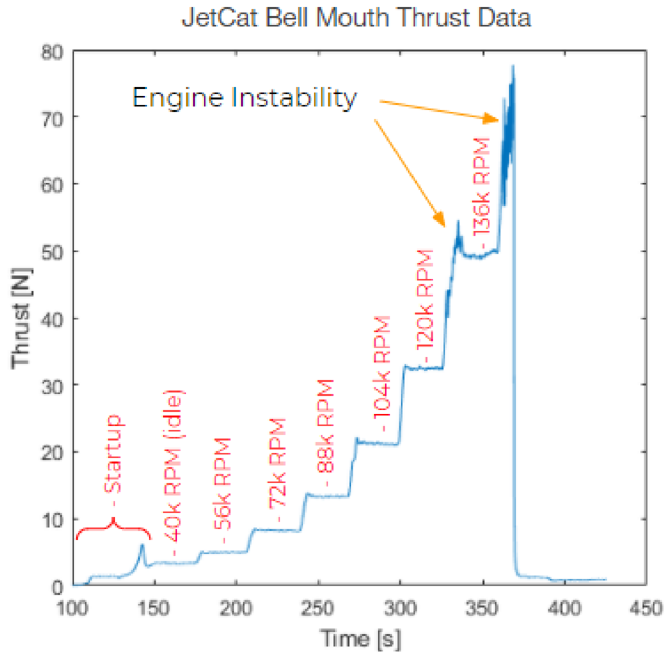


Figure 32: JetCat Mass Flow Thrust Data

After discussing the surging issue with experts in the field of aerodynamics, it was suggested that the extreme turning angle of the AFRL transition piece may be the root cause. Below in Figure 33 it is easy to see the extreme turning angle (highlighted in yellow) for the flow in the cross section drawing of the AFRL designed transition piece. Upon talking with representatives at AFRL, a test with just the AFRL transition piece attached to the JetCat was requested. In this test, the surging phenomena was seen starting at 101k RPM, but became unstable at 127k RPM which again warranted test termination and engine shutdown. Seeing the surging issues at lower RPMs when there was only the AFRL transition piece attached makes sense as the flow from the ambient air has a tight corner to turn around at the very front of the transition piece. The bell mouth is designed to make this initial sharp turning angle into a gradual one for the flow from the ambient air reducing the undesirable turbulent flow for the compressor's face. This test confirmed that the surging issues were caused by the AFRL transition piece as the stock JetCat had none of these issues through the RPM sweep.

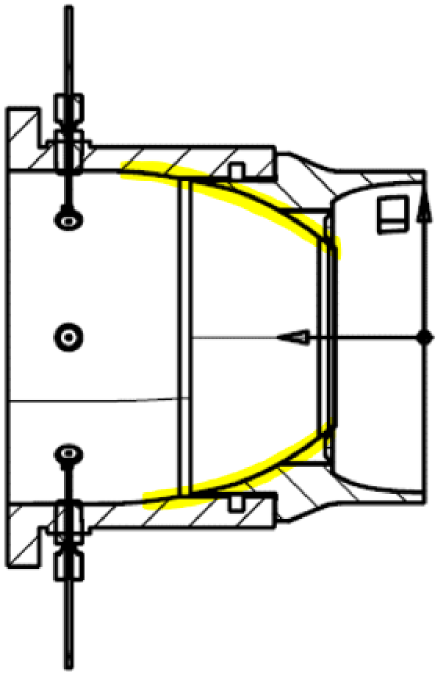

Figure 33: AFRL Designed Transition Piece Cross Section

From the results of these tests, the team set a limit of 120k RPMs for all subsequent tests. At this reduced maximum thrust, the mass flow of the JetCat P-100Rx was $0.26 kg/s$. This is in contrast to manufacture reported mass flow of $0.23 kg/s$ at the full 156k RPM. This difference in values did not have a substantial effect on the project or inlet design, but is important to note.

#### 5.3.3 Thrust Measurements

Thrust was measured using the existing test stand for the JetCat Engine. This stand included a rail-mounted sled which pushed against a load cell to measure thrust (see Figure 35). Baseline thrust data was collected using the AFRL transition piece with no inlet attached, as will be the case for final inlet testing at the APOP competition. Inlet thrust data was collected without the test apparatus frame as preliminary load cell trials revealed that this assembly introduced significant static friction. This resulted in an unacceptable uncertainty for determining the thrust decrement. To support the weight of the inlet, a small cradle was placed under the transition piece and mounted to the sled itself rather than the static part of the test stand. This cradle, printed in teal PLA, can be seen in Figure 36. Additionally, to correctly account for friction, a calibration was performed immediately prior to each test using the pulley system shown in Figure 34. This pulley used a delrin bushing on a polished steel shaft to reduce the frictional moment and ran the cord over a spool to provide it with mechanical advantage over that moment. Cast Iron plates with weights of 5.30 lb and 10.06 lb were used to apply a known force to the engine mounts. Known force applications were repeated several times for each weight, revealing highly repeatable force measurements on the order of hundredths of a pound. The added weight of the OSPRI inlet does appear to have increased friction, requiring a slightly larger scale factor to achieve accurate force measurements. Uncertainty increased with with increases in simulated thrust but remained fairly consistent between test setups as shown in Table 4.

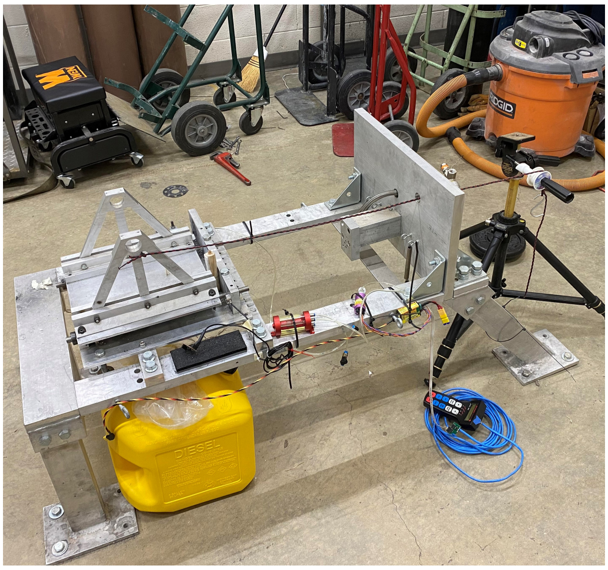

Figure 34: Load Cell Calibration Setup

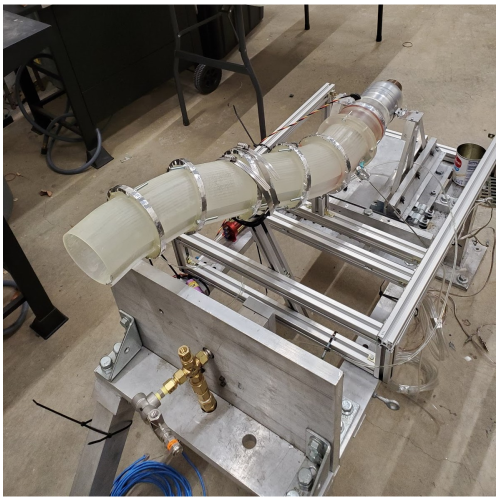

Figure 35: Initial Inlet Support Frame Design

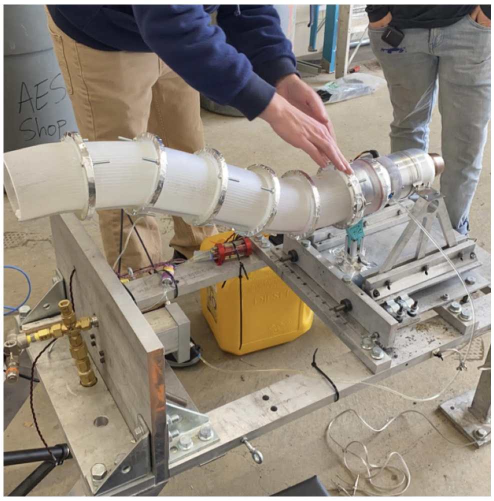

Figure 36: Updated Inlet Support Design

Table 4: Load Cell Calibration Results

| Setup | Scale Factor | $\sigma_0$ | $\sigma_5$ | $\sigma_{10}$ |
|---|---|---|---|---|
| Transition Piece Only | 0.909 | $\pm$ 0.007 lb | $\pm$ 0.027 lb | $\pm$ 0.052 lb |
| OSPRI Inlet Attached | 0.948 | $\pm$ 0.009 lb | $\pm$ 0.023 lb | $\pm$ 0.061 lb |

The calibrated and filtered thrust data is shown in Figure 37. Simple filtering was used to remove obvious outliers where the recorded thrust jumped by tens or hundreds of pounds. Additionally, occasional write errors resulted in the recorded time of a sample being incomplete, for example it may drop the first or last digit of the time. These incorrect samples were also detected and removed. It is suspected that the same mechanism may be causing the random spikes in recorded force as well. During these trials, the JetCat RPM setting was increased incrementally. Both setups were limited by an engine surging issue which is believed to be caused by the geometry of the AFRL designed transition piece. Earlier tests with a straight bell mouth inlet found that surging began at 130 kRPM so the limit was set at 120 kRPM. However, it was discovered that with no inlet attached, the AFRL transition piece produced surging at as low as 101 kRPM and thus was limited to 100 kRPM during the baseline test. The test conditions are detailed in Table 5, however, only the first four conditions allow the two setups to be compared directly.

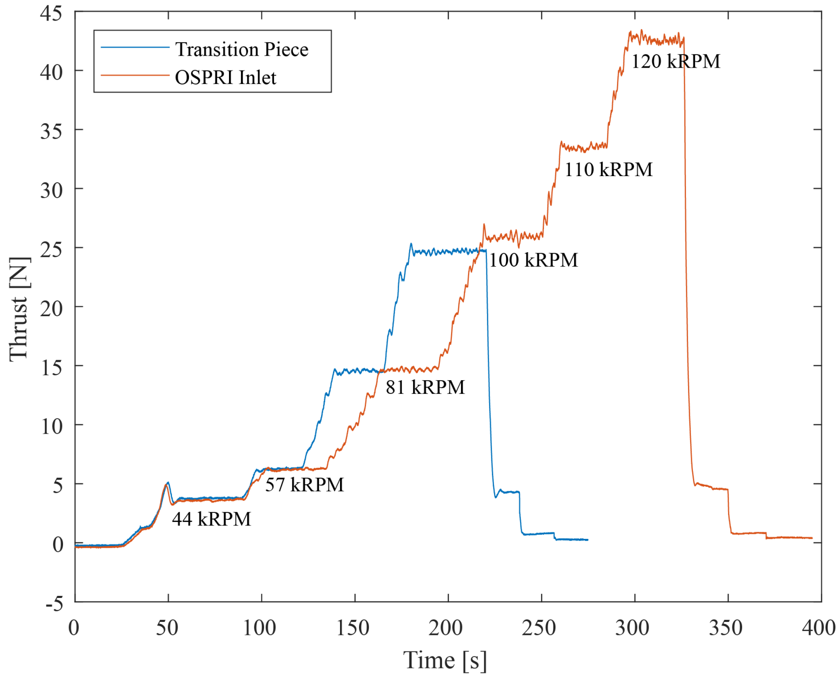


Figure 37: Filtered Thrust Data for The OSPRI Inlet and AFRL Transition Piece

Table 5: Thrust Measurement Test Conditions

| | 44 kRPM | 57 kRPM | 81 kRPM | 100 kRPM | 110 kRPM | 120 kRPM |
|---|---|---|---|---|---|---|
| AFRL | ± 300 RPM | ± 300 RPM | ± 300 RPM | ± 500 RPM | - | - |
| OSPRI | ± 400 RPM | ± 300 RPM | ± 500 RPM | ± 300 RPM | ± 200 RPM | ± 300 RPM |

The thrust data was analyzed at each RPM setting for a ten second period corresponding to about 385 samples. The data is condensed into two thrust curves shown in Figure 38. It is clear that the variations in RPM, as listed in Table 5, are very small at this scale. Error bars for the thrust data are at 3 times the standard deviation corresponding to a 99.7% certainty. The variability in the sample data is very small, thus the primary contributor to this uncertainty came from the calibration results detailed in Table 4. From the thrust curve plot it appears that the transition piece outperforms the inlet at low RPM settings but the inlet sees higher thrust at the maximum setting.

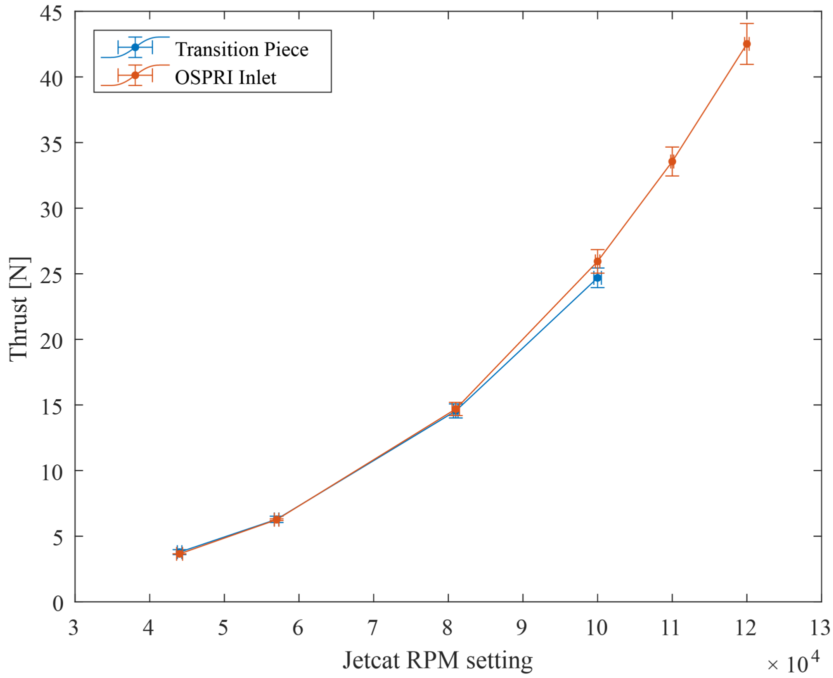


Figure 38: Thrust Curve With and Without OSPRI Inlet

Figure 39 shows the difference in thrust as a percentage of the baseline value. This is the metric that AFRL wishes to investigate and should not go bellow -5% to satisfy their requirements. The worst decrement is observed at idle with a value of -3.459% ± 1.647%. This implies that the thrust decrement requirement is very likely to be satisfied. The change in thrust improves with increasing RPM reaching a value of +5.074% ± 1.575% at the maximum RPM setting. This implies, with great certainty, that the OSPRI inlet is able to outperform the AFRL transition piece at operational RPM values. While not the expected outcome, this is not unreasonable. Both the OSPRI inlet and the AFRL transition piece have relatively sharp corners at their entrances which is not ideal for smooth turning of the flow. The OSPRI inlet has a very small radius rather than a 90° corner which may slightly improve its performance, however, it's believed that the additional length of the OSPRI inlet is the primary contributor to this improved performance. This added length provides more area for the flow to stabilize after this harsh turn, as was seen during EDF testing. Flow separation at the entrance is most significant at high RPM values due to the increased mass flow, however, OSPRI's conservative design ensured that airflow was stable by the time it reached the transition piece, improving thrust and delaying the surging issue from 101 kRPM to 130kRPM. In this area, the inlet achieved and surpassed its maximum level of success.

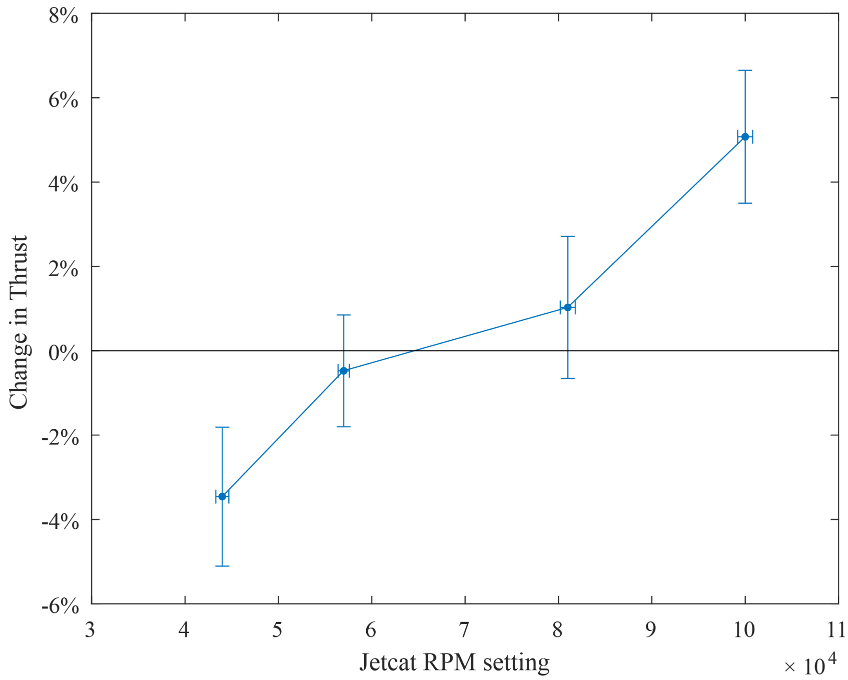


Figure 39: Effect Of The OSPRI Inlet on Thrust Compared to the AFRL Transition Piece

### 5.4 Total Pressure Recovery with JetCat Testing

The total pressure recovery for the inlet attached to the jet engine was 99.98%, when compared to the EDF, they are almost the same, with the EDF total pressure recovery at 99.8%. The CFD model predicted that the total pressure recovery would be approximately 99.98%. Which as mentioned before, is likely due to the model considering the flow as incompressible and only subtracting the boundary layer flow slow-down. This fullfills AFRL's requirement of having a total pressure recovery of greater than or equal to 98%.

## 6 Risk Assessment and Mitigation

### 6.1 Inlet Design Risks

The main risks identified for the current inlet design are listed below along with their mitigation strategies and risk matrix:

1. Inlet Material Failure
2. Flow Soiling Effects
3. Flow Leakage through Surface or Integration with TA

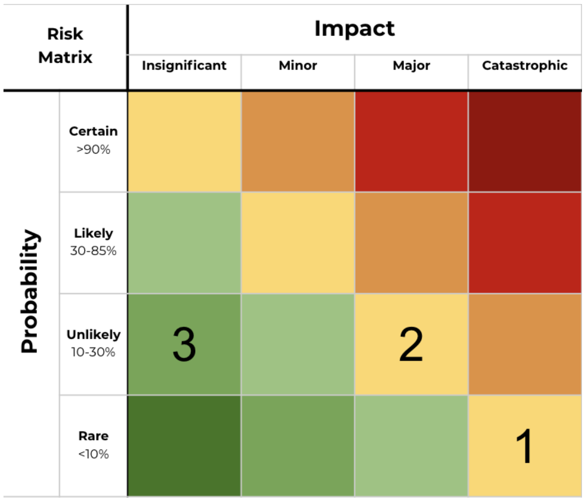


Figure 40: Inlet Design Risk Matrix

Listed below, in order, are the risk mitigation strategies identified to ensure the inlet can fulfil its design requirements:

1. The first major risk considered with regard to the inlet design was material failure. When attached to the EDF or JetCat engine, the inlet must be able to support itself and maintain functionality as it is tested. To mitigate material failure, the inlet thickness would be increased to dampen the fragility of the inlet. This will ensure the inlet has the proper material strength to support itself as experiments are conducted. This risk had no effect on the success of the project, as the inlet material was able to support itself while attached to the engine and EDF.

2. Total pressure recovery and internal flow quality are paramount to the success of this project, and as a result, soiling effects are a potential risk. To assist in the mitigation of poor internal flow quality, vortex generators have been proposed as a solution. Installed in a circumferential pattern around the inside of the inlet, the vortex generators have the capacity to decrease flow separation around the corners and bends in the inlet while also maintaining the proper mass flow for optimal engine performance. Vortex generators cannot be modeled in CFD, so their exact placement within the inlet will be determined via a trial and error method; placing them at 10%, 20%, 30% etc of the inlet length to determine the best location. This risk did not end up being a large concern for the team, since we consistently obtained reliable pressure recovery data indicating our $\geq 98\%$ margin was satisfied.

3. The final risk identified for the inlet is flow leakage through the inlet surface or leakage through integration with the test apparatus. With the utilization of the slotted inlet concept, there will be a small gap running down the length of the inlet to make room for the adjustable pitot probe for pressure measurements. This gap poses a risk to the inlet's pressure recovery and mass flow during testing and verification. To mitigate this risk, the short term solution will be to use HVAC or aluminum tape to cover the gap and prevent flow leakage. The long term solution will be to re-manufacture the inlet with discrete points for the pitot probe placement should the slot prove to be a substantial threat to flow quality and pressure recovery. This risk was also not a hindrance to the success of the project. Aluminum tape covering potential gaps was more than sufficient to prevent flow leakage through the inlet.

## 6.2 Test Apparatus Design Risks

A wide variety of risks have been identified and considered for the current test apparatus design. Of most significance and discussed in further detail below are:

1. Short EDF battery duration and performance
2. Too little mass flow from EDF surrogate
3. Inaccurate EDF mass flow control
4. Non-negligible error introduced with slotted inlet concept
5. JetCat engine unable to function for testing
6. Turbine damage to compressor blades with test inlet

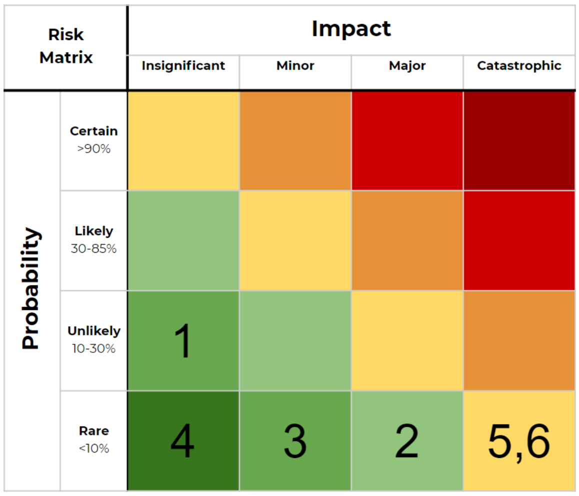


Figure 41: Test Apparatus Risk Matrix

Above is the risk matrix for the identified risks. The location of the risks in the matrix are with the associated mitigation plans that are discussed below in respective order:

1. Considered first was the testing times possible using a LiPo battery to drive the EDF. Currently under consideration is a 6 cell (22.2V) LiPo battery with a capacity of 22000mAh provided by the ASEN department. At a maximum amperage draw of 53A for our selected EDF this battery would allow testing times of up to around 25 minutes at a minimum, as we would be testing a range of RPMs and not continuously at full throttle. While this should be sufficient, in order to mitigate the risk of this testing time being insufficient, the possibility of utilizing two 24V car batteries in series, with a total capacity of around 110000mAh is also available to us and would allow for testing times of around 2 hours for full throttle tests. The risk of insufficient testing times has been considered to have a fairly insignificant impact on the overall project and is unlikely to occur. This ultimately had no effect of the success of the project, as the battery proved to have sufficient capacity for our testing purposes.

2. The EDF that was chosen as a mass flow surrogate for the JetCat Engine was the E-flite Delta V32 with a mass flow rate of 0.36kg/s. If this mass flow is not enough to replicate the mass flow of the turbine engine in real world testing, there are larger EDFs (up to 120 mm) that can be purchased in order to provide more mass flow through the test inlet. The E-flite Delta V32 proved to have the required mass flow characteristics to accurately model the JetCat engine performance metrics, and did not effect the success of the project.

3. In order to simulate engine conditions, the flow rate, and as such the RPM of the EDF, must be consistent when controlled using input amperage from the ESC. In case this method is not accurate enough, the possibility of implementing an RPM sensor into the EDF and a control loop into the LabView VI is the most promising mitigation of this issue. The myRIO is capable of handling multiple additional analog inputs, while a light gate or hall effect sensor can easily be integrated into other EDF and provide accurate RPM readings. The risk of inaccurate and inconsistent mass flow rate control on the EDF is considered to be a rare occurrence with minor effects on the project after mitigation strategies. This risk ended up not being an issue, since the EDF was instead controlled with an oscilloscope driven with duty cycle commands from 5-10%. This proved much more reliable than using LabView or the myRIO. This ended up not posing the project any detriment to its success.

4. Another concern is the slot in the slotted inlet design causing large discrepancies in the pressure readings (relative to analytical and CFD models) during verification of the test apparatus and the verification inlet prototype. In order to mitigate issues of this nature the slot will be designed to the minimally possible width which would still allow the pitot probe to have the required freedom of movement. The likelihood of this occurring was categorized as unlikely after further research but the effect would be rather significant. If this were the case our testing methodology would have to be adjusted for detection of flow distortions. As such, a discrete measurement methodology would

be implemented with varying locations for the pitot probe to be placed. These locations would much more easily be covered to avoid flow effects. With this mitigation strategy, the risk of the slotted inlet design affecting the flow characteristics would be completely avoided and would only cause a manageable inconvenience in the data collection process. At the end of testing, no large discrepancies in pressure were found due to the slotted design. As such, this risk did not influence project success.

5. The final concerns are relevant only to live turbine engine tests. The first of these concerns is a malfunctioning JetCat turbine engine. In past projects, these turbine engines have been known to be extremely finicky and hard to keep running. In an effort to combat this, a member on the team has extensive experience with these turbine engines and is in charge of all turbine testing. In order to mitigate any engine related problems, the JetCat engine has been sent to the JetCat service center to have experts properly identify issues and ensure the engine is in working order. Additionally, more turbine ground support equipment that is recommended from the manufacture will be bought in order to increase the reliability of the engine. During testing, the engine was experiencing surging issues at around 130k RPM. This did pose a hindrance to the success of this project, since this surging effect limited our operational range for the engine. As a result of this, engine performance could only be tested to 120k RPM instead of the full RPM sweep.

6. Other concerns regarding live turbine engine tests are damage to the engine's compressor blades or other components and the catastrophic failure of the engine. In order to mitigate these issues, all test with prototype inlets will be conducted with the EDF as a mass flow surrogate. In case of damage to the EDF it can cheaply be replaced and in case of a catastrophic failure will not have the potential of exploding. The major concern of FOD from early prototype 3D printed inlets can be mitigated by this method and testing with the live engine will only commence once the inlets have been determined to be structurally sound. Furthermore, in case of any damage that is not cause directly by our actions, such as a malfunction with the electronics, the team is in close contact with a JetCat maintenance team in the US which can relatively cheaply and quickly handle any repair jobs. As such, engine FOD is extremely unlikely in the controlled conditions in which we will be testing with a live engine, and while engine malfunctions may be less rare our available contingency plan allows this risk to be only have minor impacts on project schedule and costs.

# 7 Project Planning

Team OSPRI's project management process was based on a program management approach with semi-weekly meetings. The team was split into two smaller sub-teams: Inlet and Test Apparatus. These sub-teams then had sub-team leads selected, and they operated as project managers for their respective sub-teams. At each meeting, the sub-teams gave a run-down of the progress since the last meeting in order to keep the entire team up-to-date on project progress. Initially, slides were made for each meeting, typically the morning of, and they would set the agenda.

The project manager for Team OSPRI worked with the sub-team leads to delegate major tasks and deadlines, and left minor task assignment to the sub-team leads. In addition to these sub-team leads, each member of Team OSPRI had a leadership role assigned to them. The organizational chart presented in the Fall Final Report has been reproduced below in Fig. 42. The assignment for each sub-team can also be found in Figs. 43a and 43b.

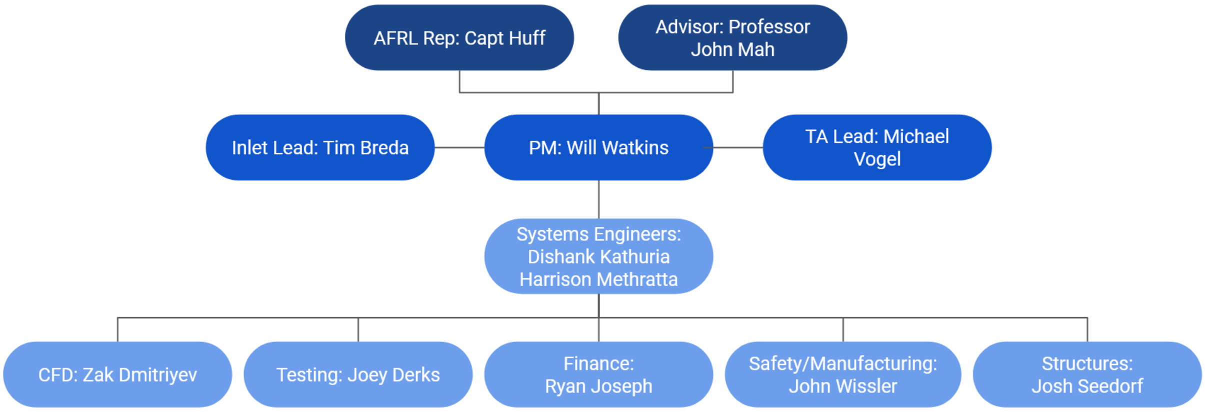


Figure 42: Team OSPRI Spring 2021 Org Chart.


(a) Fall 2020 Inlet Sub-team.

(b) Fall 2020 TA Sub-team.

Figure 43: Team OSPRI Fall 2020 Sub-team Breakdown.

However, changes were made over the winter break to this organizational chart, seen in Fig. 44. Dishank Kathuria took over the Inlet Sub-team Lead position, while Tim Breda switched to Safety/-Manufacturing with John Wissler. Michael Vogel and Joey Derks also switched positions, with Joey taking over the Test Apparatus Sub-team Lead, and Michael assuming command of Testing. These changes were made after identifying additional strengths in the team members, and the org chart was reworked to have the most efficiently-run team. After the design phase of the inlet was finished, the sub-teams were also re-tooled to allow the Test Apparatus team to distribute work items better. These new sub-teams are seen in Figs. 45a and 45b.

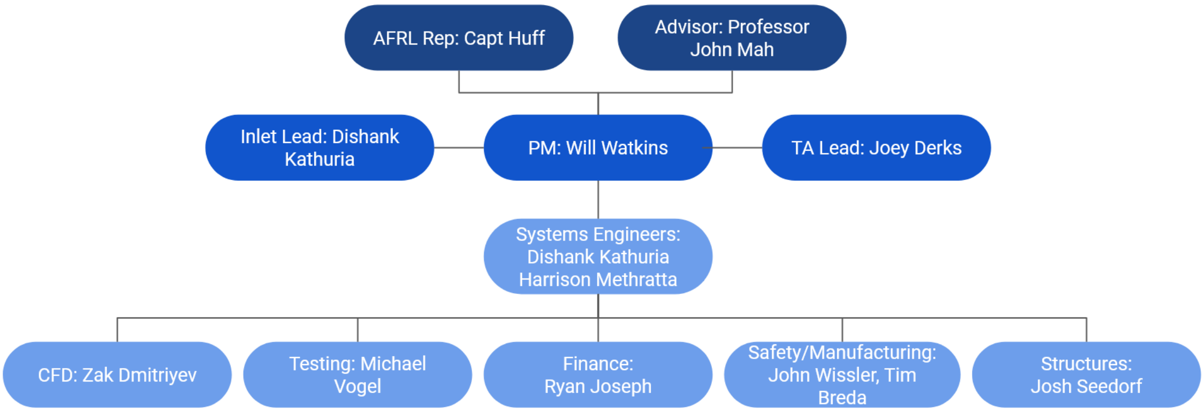


Figure 44: Team OSPRI Spring 2021 Modified Org Chart.


(a) Spring 2021 Inlet Sub-team.

(b) Spring 2021 TA Sub-team.

Figure 45: Team OSPRI Spring 2021 Sub-team Breakdown.

The top level Work Breakdown Structure (WBS) is outlined in Figure 46. Throughout the year, the team was broken into four primary categories: Project Management, Inlet, Test Apparatus, and the JetCat Engine.

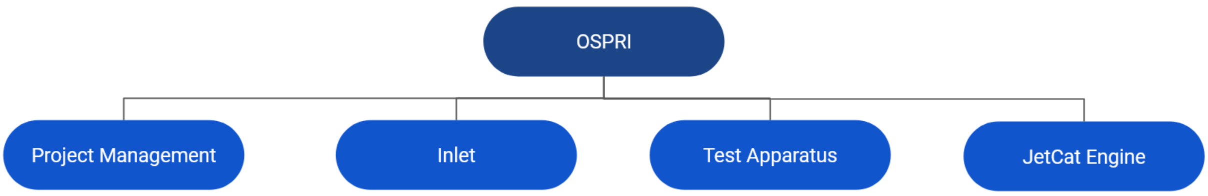


Figure 46: Team OSPRI Work Breakdown Structure

Project Management focused on the deliverables for the ASEN 4018/28 course, including, but not limited to, the Project Definition Document, the Conceptual Design Review, and the Spring Final Review. A complete list can be found in Fig. 47a. The Inlet category focused on designing, producing, and then analyzing the s-duct inlet for Team OSPRI, as seen in Fig. ??. Of note is a change in one of the work breakdown tasks: the data analysis for the inlet was moved from the Test Apparatus team to the Inlet team. Test Apparatus tasks consisted of the design, assembly, and verification of the test apparatus, and the WBS can be found in Fig. 47c. Finally, tasks for the JetCat Engine have also been broken out in the WBS because of the importance of having a running engine. This category is focused on getting the stock JetCat P100-RX engine running again, and specific tasks can be found in Fig. 47d.

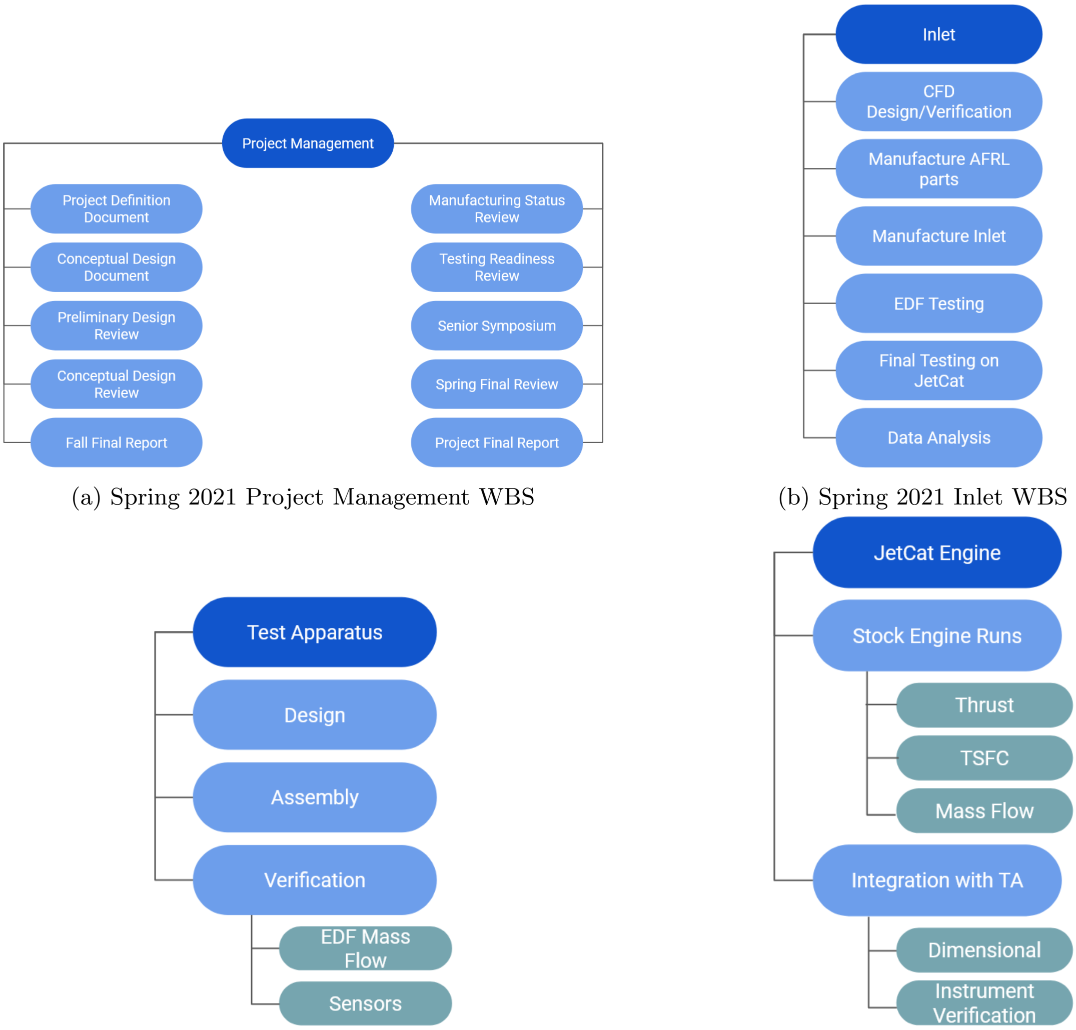


(a) Spring 2021 Project Management WBS

(b) Spring 2021 Inlet WBS

(c) Spring 2021 TA WBS

(d) Spring 2021 JetCat WBS

Figure 47: Team OSPRI Sub-team Work Breakdown Structures.

Team OSPRI used a GANTT chart for assigning and scheduling work tasks throughout the year, adding and subtracting as necessary. The Work Plan for the Fall 2020 semester is in Fig. 48, and for Spring 2021 in Fig. 49. The Fall 2020 Gantt chart was reproduced from the Fall Final Report, and the Spring 2021 Gantt chart details the final timeline that Team OSPRI used.

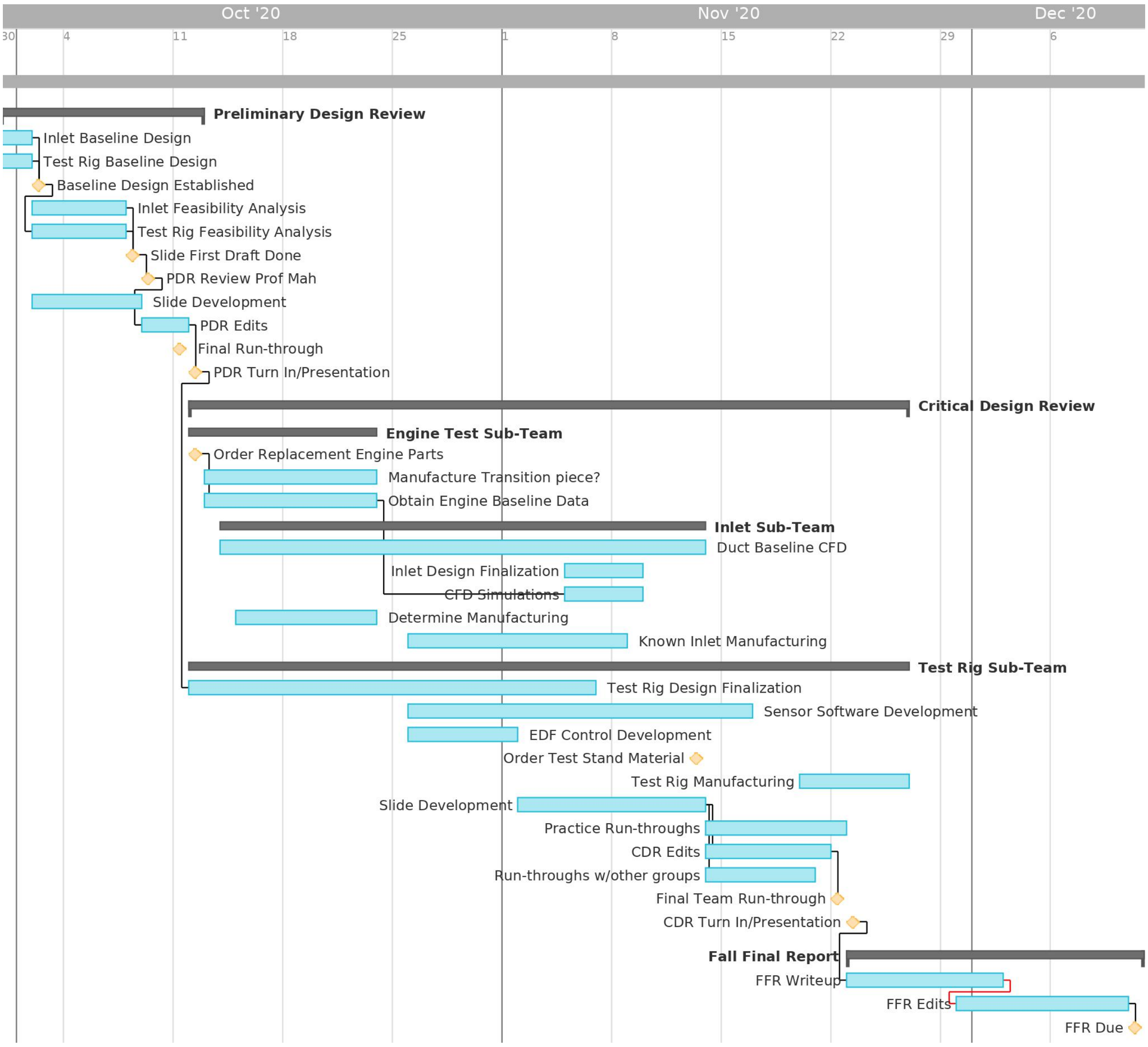


Figure 48: Team OSPRI Fall 2020 Gantt Chart

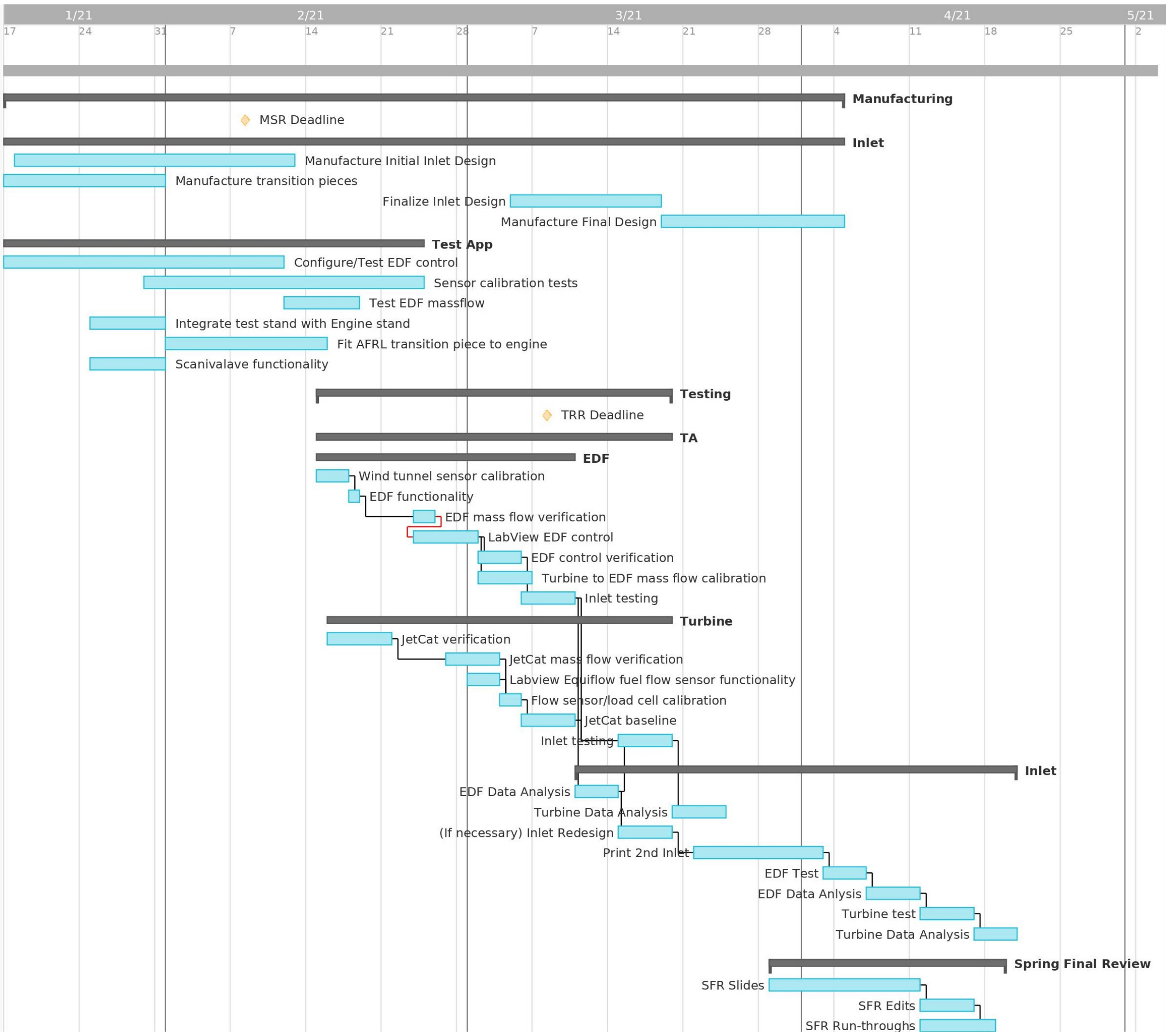


Figure 49: Team OSPRI Spring 2021 Gantt Chart

Team OSPRI's budget has been reproduced in Fig. 50. The total spent was $3,500.9. This was almost exactly 70% of the $5,000 that was allocated to the team, and nearly exactly what had been budgeted at the beginning of the Fall 2020 semester. $1,500 was left unused by the end of the semester. Below is the final budget breakdown of how the team's funds were allocated.

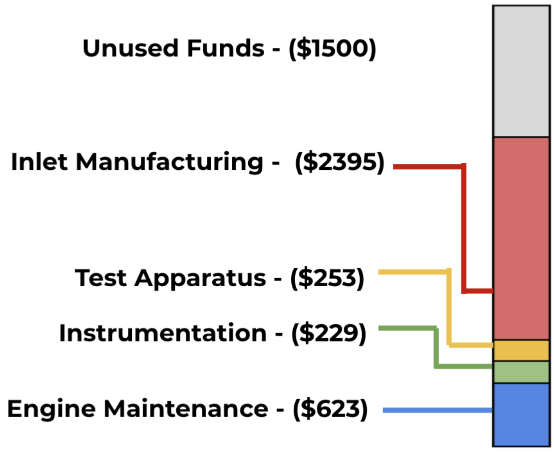


Figure 50: Team OSPRI Cost Plan

Finally, the Test Plan for Team OSPRI is shown below. Building access and engine cell access were obtained by emailing the building manager and the room manager.

| System 1: EDF testing | | | | | |
|---|---|---|---|---|---|
| Task number | Due date | Task/description | Dependent on task: | Building access required | Complete |
| E.1.a | 24 Jan | EDF transition piece design/print | N/A | N | Y |
| E.1.b | 24 Jan | EDF/Transition Piece cradles design/print | N/A | N | Y |
| E.1.c | 24 Jan | Bell Mouth design/print | N/A | N | Y |
| E.1.d (TA.1) | 24 Jan | Inlet frame assembly | N/A | N | Y |
| E.2 (TA.2) | 31 Jan | Labview scannivalve functionality | N/A | Y | Y |
| E.3 (TA.3) | 3 Feb | Wind tunnel sensor calibration test | E.2 (TA.2) | Y | Y |
| E.4 | 5 Feb | EDF systems functionality test with temporary control and frame integration | E.1 | - | Y |
| E.5 | 10 Feb | EDF mass flow verification test | E.1, E.2, E.3, E.4 | Y | Y |
| E.6 | 12 Feb | Labview EDF control functionality | E.4 | N | Y |
| E.7.a | 19 Feb | EDF control verification tests | E.6, J.5 | N | Y |
| E.7.b | 19 Feb | Turbine to EDF mass flow calibration tests | E.1, E.2, E.3, E.4 | Y | Y |
| E.8 | 19 Feb | Inlet testing | E.1-E.8 | Y | Y |

| System 2: JetCat Turbine testing | | | | | |
|---|---|---|---|---|---|
| Task number | Due date | Task/description | Dependent on task: | Building access required | Complete |
| J.1.a | 24 Jan | AFRL transition piece print | N/A | N | Y |
| J.1.b | 24 Jan | Bell mouth design/print | N/A | N | Y |
| J.1.c | 24 Jan | Transition piece print | N/A | N | Y |
| J.1.d (TA.1) | 24 Jan | Inlet frame assembly | N/A | N | Y |
| J.3 (TA.2) | 31 Jan | Labview scannivalve functionality | N/A | N | Y |
| J.4 (TA.3) | 3 Feb | Wind tunnel sensor calibration test | J.3 (TA.2) | Y | Y |
| J.2 | (Org 27 Jan ) 15 Feb | JetCat verification run | N/A | Y | Y |
| J.5 | 15 Feb | JetCat mass flow verification test | J.1, J.2, J.3, J.4 | Y | Y |
| J.6 | 21 Feb | Labview Equiflow fuel flow sensor functionality | N/A | N | N |
| J.7 | 24 Feb | Flow sensor/load cell calibration test | J.6 | Y | Y/N |
| J.8 | 26 Feb | JetCat baseline test | J.3, J.4, J.5, J.6, J.7 | Y | Y |
| J.9 | 26 Feb | Inlet testing | J.1 - J.8, E.8 | Y | Y |

Figure 51: Team OSPRI Testing Outline

# 8 Lessons Learned

## 8.1 Engineering

### 8.1.1 Inlet Design

The inlet designed by OSPRI met the customer requirements. However, the designed inlet is conservatively long which enables it to perform extremely well. If it was to be redesigned, decreasing the horizontal length would be the first change that would be implemented. Due to time constraints, Team OSPRI was unable to carry out any further design changes in order to test a shorter inlet which would have resulted in more points at the APOP competition.

### 8.1.2 Inlet Manufacturing

For inlet manufacturing, Stereolithography(SLA) 3D printing was used. This allowed for cheaper and faster manufacturing since it was all done in house in the Aerospace Machine Shop. Although, it came with a few problems. In order to fit the printer, the inlet had to be divided into sections which caused some inconsistencies when assembling due to printer margins. Additionally, the post processing took extra days and care since the support structure had to be removed. Ideally, the inlet would be printed/manufactured as one whole piece which would remove any inconsistent surfaces. For that, exploring new ways to manufacture like sheet bending, fiberglass molding etc. would result in a more cleaner inlet.

### 8.1.3 Test Apparatus Design and Assembly

The test apparatus was designed to accommodate any inlet design which it was very capable of doing. Engine and inlet tests were performed successfully on the designed test apparatus. However, the integration of the test stand with the inlet was time consuming and physically exhausting as the bolts and bars used were not easily adjustable and required intense force to re-position. Moreover, during the engine test integration, it wasn't able to accommodate the pitot tube in its original configuration. The inlet had to be titled in order to rectify this issue as seen in Fig. 52.

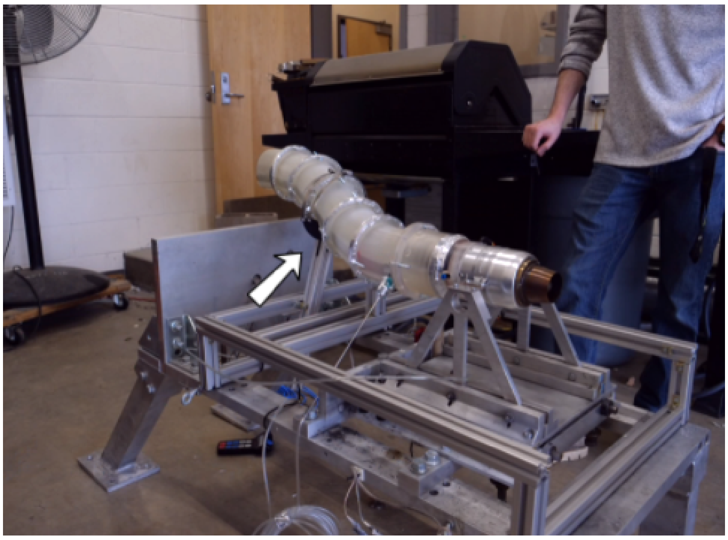

Figure 52: Tilted Inlet for Pitot Adjustment

For a future iteration of the test apparatus, the design would focus around easily adjustable parts that are based on push and click parts compared to screwing in for the current generation. This will save a significant amount of time and manpower.

#### 8.1.4 Data Collection and Sensor Calibration

One of the primary lessons learned during testing was the importance of calibration and error minimization for load cell measurements. Figures 53 and 54 show thrust results from three early turbine tests. The red and blue lines in both Figures represent two tests of the same inlet on the same day but with a different pitot-static probe location. We should not expect substantial thrust variance between these trials, however, they differ by up to 10%. This uncertainty was unacceptable for determining whether the thrust decrement criteria, less than 5%, was met. The cause of this was determined to be static friction caused by the test apparatus frame used to support the inlet. In Figure 53 the load does not return to zero after termination of the second inlet test, indicating that the stand slipped and became stuck in it's new position due to static friction. This introduced additional preload to the load cell resulting in a positive force after shutdown. Static friction would also have impacted the first inlet test, and the baseline bell mouth test, resulting in unreliable data.

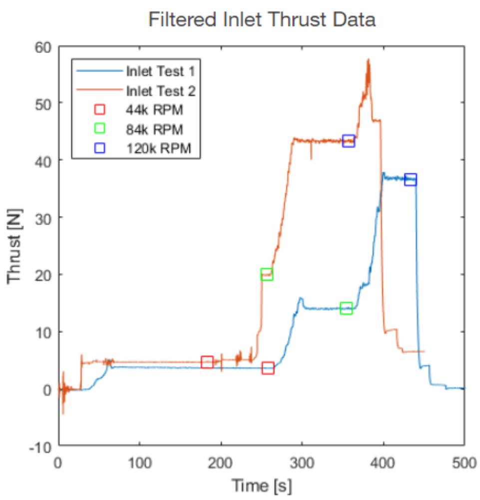


Figure 53: Thrust vs Time Plot

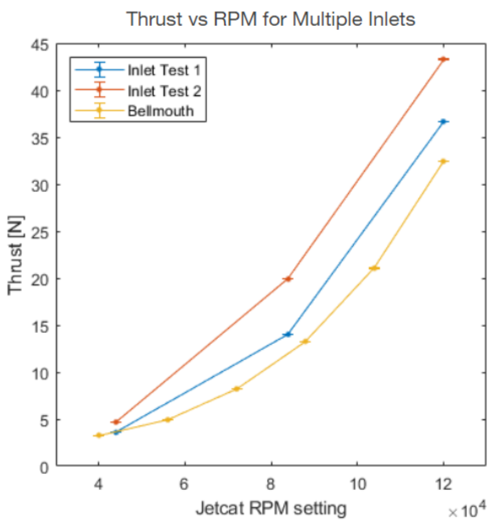


Figure 54: Thrust vs RPM Plot

These unexpected errors could have been prevented if load cell tests were conducted earlier in the project using known forces as described in Section 5.3.3. Even without a functional engine, calibration of the sensor could have been performed to ensure accurate absolute force measurements and provide the team with a better understanding of the uncertainties. Had these tests been conducted earlier, the modified support structure could have been used during the pressure recovery tests, eliminating the need for a repeat testing near the end of the semester. Additionally, it was important to calibrate the load cell prior to each test as each setup had a slightly different scaling error depending on the loads and moments being applied to the sled. In the future, calibrating all sensors would be the first task on the agenda before any testing in order to avoid retesting due to inconsistent data.

## 8.2 Project Management

While Team OSPRI did make timely progress, there were some growing pains and mistakes as the academic year progressed. After the first month, the specificity of project management products fell off. That is, the semi-weekly meeting slides stopped being produced, as making them the morning of was taking too much time, and there was no "pre-staging" a template for each subsequent week. At the same time, the written meeting schedules started to slip, and they became mostly word-of-mouth rather than hard agenda items. This resulted in less than 100% efficient team meetings, wasting time and effort in the process. In addition to this, the Gantt chart fell behind the actual project schedule. Like with the meeting schedules, task and team assignments were largely done via word-of-mouth, and there were a number of times that team members were unsure of what they were supposed to be doing or when a certain task was due by. In the end, communication breakdown was at the core of the problems that Team OSPRI faced throughout the year.

As far as lessons learned from these missteps, the most obvious one is to be more diligent in updating project management products. By updating the Gantt chart, meeting slides and meeting agenda, and then distributing these to the team, most of the confusion would have been eliminated. Additionally, using meeting slides only once per week would have lightened the load on the project manager, and would've been more than adequate as formal updates were not necessary more than once per week throughout the school year. Better communication is the key to most of the issue Team OSPRI faced, but more specifically, better follow-up would have alleviated the last minute scramble the team faced quite often. This must be done in such a way that team members do not feel micro-managed, but the schedule is still being adhered to.

The most important lesson, however, is to know when help is required. Project Management advice was sought out at the beginning of the Fall 2021 semester from an expert in the field with more than 30 years of experience. This advice worked well for the first month or two of Team OSPRI's project. However, once the team fell off the proverbial bandwagon, the correct decision would've been to seek out that expert again, and determine how to course correct back and stay on the right path. Unfortunately, this did not happen, and instead the project manager followed the flawed plan outlined previously.

# 9 Individual Report Contributions

The role of each group member is detailed below:

- **William Watkins:** On the Project Final Report, William produced the project management sections, namely Sections **1** (Project Purpose and Overview), **2** (Project Objectives and Functional Requirements), **7** (Project Planning), and **8.2** (Lessons Learned: Project Management). Throughout the academic year, William functioned as the project manager for Team OSPRI.

- **Dishank Kathuria:** On this report, Dishank focused heavily on section **8**(Lessons learned) and overall editing of the report. During the semester, Dishank lead the inlet team where he was responsible for design verification, and CAD development of the inlet. In addition the inlet team, Dishank was also the systems engineering lead where he played a key role in making sure the inlet and the transition piece interfaced with the test apparatus. Dishank was also responsible for developing the demonstration video for Team OSPRI.

- **Harrison Methratta:** For OSPRI's Project Final Report, Harrison was responsible for writing sections **4.2** (Test Apparatus Manufacturing), **6.1** (Inlet Design Risks), **6.2** (Test Apparatus Design Risks). Throughout the semester, Harrison was involved with designing the pressure data acquisition system, as well as EDF & JetCat baseline testing, inlet & EDF integration testing, and JetCat & inlet integration testing. Harrison worked closely with Josh Mellin this semester on designing and understanding data acquisition code and Scanivalve hardware/software development.

- **Joseph Derks:** On this report, Joseph was heavily involved in writing sections **3.3** (Test Apparatus Design), **5.1** (EDF Verification and Validation), **5.2** (Inlet Performance vs CFD Model Performance), and **5.3** (JetCat Testing). In addition to writing these sections, through the year Joseph did all the design of the inlet test frame, lead the testing and maintenance of the JetCat turbine engine, lead the brainstorming of the test apparatus risks, and lead the test apparatus team with getting testing functioning. Joseph was heavily involved in the design of the each of the tests and the overall testing scheme for the inlet on the EDF testing route and the JetCat testing route as well as securing permission to utilize test equipment and and leading the scheduling of testing facilities throughout the entire semester.

- **John Wissler:** For this report, John worked on sections **4.1** (Inlet Manufacturing) and **3** (Final Design). Throughout the semester, John was a member of the inlet design team, focusing mainly on the manufacture and assembly of the inlet itself. This included the research and selection of manufacturing methods, as well as coordinated the manufacture of both the initial and final inlet designs and the completion of the required post-processing. John also assisted in the EDF and JetCat testing, as well as the creation of the inlet 3D model.

- **Timothy Breda:** For team OSPRI's Project Final Report, Tim completed writings in sections **4.1** (Inlet Manufacturing) and **3** (Final Design). Along with these writings, throughout the semester, Tim was involved in inlet research, design, and production. Towards the end of the project, Tim was more involved in manufacturing and initial verification tests of the inlet. Tim was also involved in assisting the test apparatus team in setting up and running thrust data measurement experiments, as well as synthesizing and documenting test matrices for each inlet validation test.

- **Ryan Joseph:** For team OSPRI's Project Final Report, Ryan documented the static test frame design procedure in section **4.2** (Test Apparatus Manufacturing) as well as documented the team's expenditures over the course of the year in section **7** (Project Planning). For the past school year, Ryan has been the CFO of the OSPRI project and has been primarily responsible for tracking expenses, staying coordinated with the aerospace finance department, and making all purchases for the team including building materials, electronics, instruments, and shipping for the JetCat engine to and from the JetCat of America facility for maintenance. Ryan also assisted with the design of multiple systems incorporated in the project including the sliding pitot tube rail and test stand.

- **Michael Vogel:** For this report, Michael was responsible for writing of section **5.1**, (EDF Verification and Validation). Michael also contributed in writing and editing to most other testing related sections, such as section **3.3** (Test Apparatus Design) and section **4.2** (Test Apparatus Manufacturing). Throughout this semester Michael's primary focus has been EDF related items and testing, leading the EDF testing efforts and assisting in any electronics related concerns.

- **Joshua Seedorf:** For this report, Josh was responsible for writing section **5.3.3** (Thrust Measurements) including all data and uncertainty analysis for load cell calibration and measurements. Additionally, he contributed to section **8** (Lessons Learned). During this final semester, Josh assisted with JetCat testing with a particular focus on achieving reliable thrust measurements. Additionally, Josh was responsible for the selection of the EDF, design of the EDF transition piece, and the design of the straight bell mouth inlet which enabled critical calibration and verification tasks.

- **Zak Dmitriyev:** Zak was responsible for writing section **3.2.1** and parts of section **5.2**, as well as some minor editing. Throughout the year, Zak handled all of the CFD analysis and workflow. Zak was also responsible for testing and verifying the inlet total pressure recovery with the EDF and the jetCat engine. Additionally, Zak conducted some emergency repairs and engineering solutions to unforeseen problems that came up during testing and verification.

# 10 References

## References


[1] Slater, J. "S-Duct Inlets" NASA NPARC Alliance Validation Archive, retrieved 10 Sep. 2020. https://www.grc.nasa.gov/www/wind/valid/sduct/sduct.html.

[2] Lockheed Martin. "The P-80 Redefines 'Fast' – In the Air and On the Assembly Line." Retrieved 11 Sep. 2020. https://www.lockheedmartin.com/en-us/news/features/history/p80.html.

[3] "A specialist performs maintenance inside the intake of an F-16 Fighting Falcon aircraft." Retrieved 12 Sep. 2020. https://catalog.archives.gov/id/6347034.

[4] Harrington-Cressman, P., "Aircraft System Compartment Diagram." Retrieved 10 Sep. 2020. https://www.airlinereporter.com/2015/09/requiem-trijet-masterpiece-lockheed-l-1011-tristar/aircraft-system-compartment-diagram/.

[5] "JetCat RX Turbines with V10 ECU." JetCat, retrieved 10 Sep. 2020. https://studylib.net/doc/18303934/jetcat-rx-turbines-with-v10-ecu.

[6] "Turbine Data Sheet." JetCat, retrieved 11 Sep. 2020. https://www.chiefaircraft.com/pdf/jetcat-data.pdf.

[7] Sanchez, A., Emmett, T., Briggs, C., Cuteri, J., Vincent, G., and Muller, A., "SABRE Project Definition Document," Sep. 2017.

[8] Harthan, D., Frank, G., Fitz-Randolph, P., Knickerboker, M., Oropeza, D., Fuernkranz, M., Piper, S., Chen, Y., Camacho, C., Junker, M., and Cutler, J., "SPECS Project Definition Document," Sep. 2018.

[9] Bosshart, A., Murray, D., Zellmann, N., Griffin, I., Sheffer, L., Witte, Z., Weidner, J., Kincaid, J., Meikle, A., Robins, A., Zardini, L., and Paquin, A., "WHiMPS Project Definition Document," Sep. 2019.

[10] Hamstra J., and McCallum, B., "Tactical Aircraft Aerodynamic Integration" Encyclopedia of Aerospace Engineering 2010 retrieved 9 Sep. 2020. https://onlinelibrary.wiley.com/doi/pdf/10.1002/9780470686652.eae490.

[11] Shu, S., Hui-jun, T., "Flow Characteristics of an Ultracompact Serpentine Inlet with an Internal Bump," 2018.

[12] Saied, E., Carl, T., Aaron A., John, W., "Experimental Investigation of Inlet-Combustor Isolators for a Dual-Mode Scramjet at a Mach Number 4," May 1995.

[13] Amer, A., Ron, B., Peter, L., "An Experimental Study of the Effect of Offset on Thick Boundary Layer Flowing Inside Diffusing Ducts," AIAA, July 1999.

[14] Amer, A., Ron, B., Peter, L., Robert, L., "An Experimental Investigation of Boundary Layer Ingestion in a Diffusing S-Duct With and Without Passive Flow Control," AIAA, Jan. 1999.

[15] Bobby, B., Melissa, C., Brian, A., "High Reynolds Number Investigation of Flush-Mounted, S-Duct Inlet With Large Amounts of Boundary Layer Ingestion," Sep. 2005.

[16] Michelle, M., Scott, M., Abe, G., Matthew, L., Ari, G., Mori, M., "Inlet Flow Control and Prediction Technologies for Embedded Propulsion Systems," Dec. 2011.

[17] Cengel, Y.A., Cimbal J.M., Turner, R.H., "Internal Flow," *Fundamentals of Thermal-Fluid Sciences,* 5th edition, Mc Graw Hill, New York, 2017.

[18] Anderson, J.D. Jr, "Inviscid, Incompressible Flow," *Fundamentals of Aerodynamics,* 6th edition, Mc Graw Hill, New York, 2017.

[19] Heinemann T., Blakeberg C., Lienhart H., Becker S., "Total Pressure Measurements Behind an Axial Ventilator Using a Kiel Probe Array," Numerical and Experimental Fluid Mechanics IX pp 573-581, 25 Jan. 2014.

[20] "Anemometer," Encyclopedia Britannica, 18 Oct. 2013, Retrieved 25 Sep. 2020. https://www.britannica.com/technology/anemometer.

[21] "30x30 Aluminum Extrusion - 6 Series, Base 30 (MISUMI)." MISUMI, us.misumi-ec.com/vona2/detail/110302686450/.

[22] "Aluminum Extrusion Types and Parts Selection." MISUMI, https://us.misumi-ec.com/pdf/fa/2012/p2_0493.pdf.

[23] Mattingly, Jack D., and Boyer, Keith M., "Elements of Propulsion: Gas Turbines and Rockets," 2nd ed., AIAA, 2016.

[24] E-flite, "Delta-V 32 80mm (EFLDF32) Fan Unit Instructions." Horizon Hobby, retrieved 11 Nov. 2020. https://www.horizonhobby.com/on/demandware.static/-/Sites-horizon-master/default/dwbee6f755/Manuals/EFLDF32-Manual-MULTI.pdf.

[25] Dwyer, "Series 160 Stainless Steel Pitot Tubes Specifications - Installation and Operating Instructions." ITM Instruments Inc., retreived 11 Dec. 2020. https://www.itm.com/pdfs/cache/www.itm.com/167-6/manual/167-6-manual.pdf.

[26] Breda, T., Derks, J., Dmitriyev, Z., Joseph, R., Kathuria, D., Methratta, H., Seedorf, J., Vogel, M., Watkins, W., and Wissler, J., "OSPRI Project Definition Document," Sep. 2020.

[27] Breda, T., Derks, J., Dmitriyev, Z., Joseph, R., Kathuria, D., Methratta, H., Seedorf, J., Vogel, M., Watkins, W., and Wissler, J., "OSPRI Conceptual Design Document," Sep. 2020.

[28] Breda, T., Derks, J., Dmitriyev, Z., Joseph, R., Kathuria, D., Methratta, H., Seedorf, J., Vogel, M., Watkins, W., and Wissler, J., "OSPRI Preliminary Design Review," Oct. 2020.

[29] Breda, T., Derks, J., Dmitriyev, Z., Joseph, R., Kathuria, D., Methratta, H., Seedorf, J., Vogel, M., Watkins, W., and Wissler, J., "OSPRI Critical Design Review," Nov. 2020.

# 11 Appendices

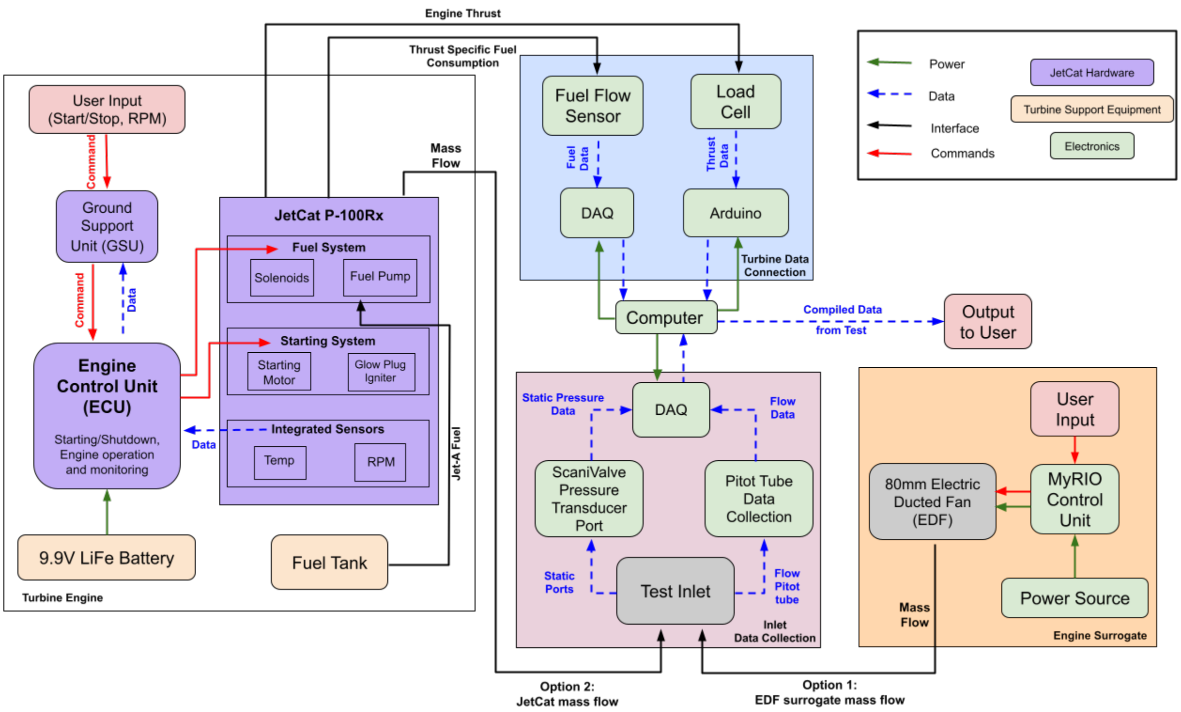


Figure 55: Testing Functional Block Diagram